



Contents lists available at ScienceDirect

Review of Palaeobotany and Palynology

journal homepage: www.elsevier.com/locate/revpalbo

Five million years of life history record in an uppermost Cretaceous northern Tethyan marine succession, Eastern Carpathians (Romania): Microfossil content and palaeoenvironmental assessment

Țabără Daniel ^{a,*}, Slimani Hamid ^b, Chelariu Ciprian ^{a,*}, Bindiu-Haitonic Raluca ^c, Bălc Ramona ^{d,e,g}, Csiki-Sava Zoltán ^{f,g}, Fabiańska J. Monika ^h, Misz-Kennan Magdalena ^h, Chelariu Marian ^a

^a "Al. I. Cuza" University of Iași, Department of Geology, 20A Carol I Blv., 700505 Iași, Romania

^b Geo-Biodiversity and Natural Patrimony Laboratory (GEOBIO), "Geophysics, Natural Patrimony and Green Chemistry" Research Center (GEOPAC), Department of Geology and Remote Sensing, Scientific Institute, Mohammed V University in Rabat, Avenue Ibn Batouta, P.B. 703, 10106 Rabat-Agdal, Morocco

^c Babeș-Bolyai University, Department of Geology and Research Centre for Integrated Geological Studies, 1 Mihail Kogălniceanu Street, 400084 Cluj-Napoca, Romania

^d Babeș-Bolyai University, Faculty of Environmental Sciences and Engineering, 30 Fântânele Street, 400294 Cluj-Napoca, Romania

^e Interdisciplinary Research Institute on Bio-Nano-Sciences, Babeș-Bolyai University, Treboniu Laurian 42, 400271 Cluj-Napoca, Romania

^f University of Bucharest, Department of Geology, 1 Nicolae Bălcescu Ave., 010041 Bucharest, Romania

^g Center for Risk Studies, Space Modeling and Dynamics of Terrestrial and Coastal Systems, University of Bucharest, 1 Nicolae Bălcescu Ave., 010041 Bucharest, Romania

^h Faculty of Natural Sciences, University of Silesia in Katowice, Bedzińska 60, 41-200 Sosnowiec, Poland

ARTICLE INFO

Article history:

Received 17 January 2023

Received in revised form 12 March 2023

Accepted 15 March 2023

Available online 20 March 2023

Keywords:

Dinocysts

Foraminifera

Calcareous nannoplankton

Hangu Formation

Eastern Carpathians

ABSTRACT

New biostratigraphic investigations based on palynomorphs (mainly dinoflagellate cysts), foraminifera and calcareous nannoplankton recovered from eight geological sections indicate that the Hangu Formation near the Pluton-Pipirig area (Tarcău Nappe, Eastern Carpathians, Romania), previously assigned to the Senonian–Paleocene interval, includes only uppermost Cretaceous deposits. The palynological assemblages are moderately rich, with a total of 167 well-preserved taxa. The marine palynomorphs – essentially consisting of dinoflagellate cysts (dinocysts) – are dominated by peridinioid taxa, mainly recorded in upper Upper Campanian–lower Maastrichtian deposits, and by a high-diversity assemblage of gonyaulacoid taxa during the late Maastrichtian. Marine algae and dinogymnioid dinocysts were less common. The terrestrial palynoflora is dominated by fern spores and angiosperm pollen, with subordinate gymnosperm pollen. The foraminiferal assemblages include an assortment of well-preserved agglutinated forms, present mainly in the upper Maastrichtian deposits, whereas calcareous benthics and planktonic foraminifera are rare and poorly preserved. Calcareous nannoplankton assemblages are also rare, often represented by two taxa (*Micula staurophora* and *Watznaueria barnesiae*); certain important biostratigraphic markers were found to be reworked in the analyzed deposits. Age assignments for the studied sections were mainly provided by dinocysts, through the identification of significant marker taxa and comparisons with well-calibrated Campanian–Maastrichtian dinocyst assemblages from well-dated sections and stratotypes, located mostly in the Northern Hemisphere.

Indices such as particulate organic matter (POM) composition, the relative abundance of dinocyst eco-groups, as well as agglutinated foraminiferal morphogroups, were used to reconstruct the depositional environments of the Hangu Formation from the studied area. The upper Upper Campanian–lower Maastrichtian deposits from the Pluton-Pipirig sections were mainly deposited in neritic marine conditions, although occasional redeposition of the sediments transported by turbidity currents towards deeper water settings is not excluded, either. The depositional environments evolve towards outer neritic to distal (bathyal) during the late Maastrichtian, as indicated by palynofacies constituents and by high frequencies of gonyaulacoid dinocysts and deep-water benthic foraminifera.

© 2023 Elsevier B.V. All rights reserved.

1. Introduction

Upper Cretaceous marine deposits of the Outer Moldavides nappe system (Săndulescu, 1984) are widespread in the Eastern Carpathians,

* Corresponding authors.

E-mail addresses: dan.tabara@yahoo.com (Ț Daniel), ciprian.chelariu@uaic.ro (C. Ciprian).

their biostratigraphic and paleoenvironmental features being important to decipher the geological evolution of the area.

Integrated biostratigraphic data (dinoflagellate cysts, calcareous nannoplankton, foraminifera) carried out on several geological sections close to each other that include Upper Cretaceous deposits assigned to the Outer Moldavides, used in the interpretation of a tectonic framework, are missing so far. Previous age assessments of the Upper Cretaceous formations in the Eastern Carpathians were for the first time achieved based on biostratigraphic studies of ammonite and inoceram assemblages (Joja and Chiriac, 1964; Turculeț, 1971). Subsequent age refinements for these units were based mainly on foraminifera, calcareous nannoplankton, and organic-walled dinoflagellate cysts (Ionesi and Tocorjescu, 1968; Ionesi, 1975; Olaru, 1978; Antonescu and Alexandrescu, 1979; Ion et al., 1982; Cetean et al., 2011; Bindiu et al., 2013; Roban et al., 2017; Țabără and Slimani, 2017; Țabără et al., 2017), but all these results were mainly obtained from various geological sections analyzed individually and located at great distances from each other along the Eastern Carpathian chain (see Fig. 1A).

The studied area extends between Pluton and Pîpirig (Neamț County, northern Eastern Carpathians), covers about 25 km², and contains a number of oil and gas fields discovered during the early 1980s. The local Upper Cretaceous–Eocene sandstones and calcarenite are considered reservoir rocks for hydrocarbon preservation in these oilfields (Constantinescu and Anastasiu, 2019). Nevertheless, despite the fact that they provided important quantities of oil at the beginning of their exploitation, these fields remain severely understudied. For this area, some limited geological information is provided only by the Piatra Neamț sheet (1:200,000 scale; Murgeanu and Mirăuță, 1968), which reveals a wide spread on the surface of the "Hangu beds" assigned to the Senonian–Paleocene age, represented by flysch deposits (claystones, marlstones, and calcarenites).

Therefore, the aims of our study are: (1) the establishment of the stratigraphic distribution of the dinoflagellate cysts, foraminifera, and calcareous nannoplankton taxa identified in eight sections of the Pluton–Pîpirig area, which refines the biostratigraphy of the Upper Cretaceous deposits and reveals a microfossil life history spanning approximately 5 Ma.; (2) the use of biostratigraphic data derived from our micropalaeontological investigations, to construct a detailed geological map of the Pluton–Pîpirig sector with newly acquired stratigraphic/tectonic details important for hydrocarbon explorations within the little-known oilfields identified in this area; and (3) the identification of palaeoenvironmental and palaeoecological conditions that prevailed during the depositions of the upper Campanian–Maastrichtian interval, based on microfossil and palynofacies data.

2. Geological setting

The Eastern Carpathians are a ~600 km long segment of the Carpathian Orogen, made up mainly of Jurassic to Miocene deposits forming a complexly stacked nappe structure, and stretches across the Romanian sector from the Dâmbovița Valley (their southern part) to the border with Ukraine. According to Săndulescu et al. (1981), the different Eastern Carpathian nappes can be grouped into several nappe systems, such as the Piennides, the Dacides, and the Moldavides, based on their geographic position, lithostratigraphic makeup, and time of emplacement. The innermost (and tectonically uppermost), but spatially restricted Piennides display a double, Cretaceous and Miocene tectogenesis, the centrally positioned Dacides, extending along the entire length of the Eastern Carpathians and continuing into the Southern Carpathians as well, were stacked mainly during the Cretaceous, while the outermost (and tectonically lowermost) Moldavides, restricted strictly to the eastern part of the Eastern Carpathians, suffered Paleogene–Miocene deformations (Săndulescu, 1984; Răbăgia et al., 2011).

The Moldavide nappe system corresponds to the main part of the outer Eastern Carpathians. It has been divided, based mainly on the

different tectonic phases that affected the deposits, into the Inner Moldavides (the Teleajen, Macla, and Audia nappes) that consist mainly of Cretaceous deposits thrustured during the Early Miocene, and the Outer Moldavides (the Tarcău, Vrancea, and Pericarpathian nappes) that comprise Cretaceous to Lower Miocene successions dominated by siliciclastic and carbonate turbidites, including pelagic intervals, deformed during different Middle Miocene to Pliocene tectonic phases (Săndulescu, 1984; Grasu et al., 1988; Bădescu, 2005).

The Tarcău Nappe, cropping out over an extensive area, forms the main body of the Outer Moldavides, and is structurally wedged between the Audia and Vrancea nappes (Fig. 1A). The oldest deposits of the Tarcău Nappe are Lower Cretaceous organic-rich black shales deposited in hemipelagic and turbidite facies, followed by Upper Cretaceous and Paleogene turbidite represented mainly by alternations of shales, marlstones, calcarenites and sandstones (Săndulescu et al., 1981; Melinte-Dobrinescu et al., 2015). According to the 1:200,000 scale geological map of Romania (Piatra Neamț sheet; Murgeanu and Mirăuță, 1968), the study area - stretching between the Neamț and Agapei rivers - is located in the western part of the central-northern segment of the Tarcău Nappe (Fig. 1A). In this area, the 1:200,000 map sheet only shows Coniacian–Paleocene sedimentary deposits assigned to the "Hangu beds" cropping out on the surface, without more detailed and precise chronostratigraphic and tectonic information.

The Hangu Formation, originally named "inocerams beds" (Macovei and Atanasiu, 1925), is over 1000 m thick and consists of alternating claystones, 'fucoid'-bearing marlstones, calcarenites, and sandstones (Grasu et al., 1988; Juravle et al., 2019). The 'fucoid' belong mostly to the ichnotaxon *Chondrites intricatus* (Bojar and Bojar, 2013), possibly indicating an anoxic environment.

3. Previous biostratigraphic and palaeoenvironmental research

The first palynozonation of the Campanian–Maastrichtian interval of the Eastern Carpathians was proposed by Antonescu and Alexandrescu (1979). It includes the *Cerodinium diebelii*–*Palaeocystodinium golzowense* Zone (Upper Campanian–lower Maastrichtian) and the *Deflandrea druggi* Zone (upper Maastrichtian). In addition to the marker species, other dinoflagellate cysts taxa such as *Cordosphaeridium fibrospinosum*, *Isabelidium cooksoniae*, *Palaeoperidinium pyrophorum* and *Phelodinium tricuspis*, have also been recorded.

Additional palynological results, derived from Campanian–Maastrichtian deposits of the central part of the Eastern Carpathians, were presented by Olaru (1978), who noted the dominance of the Normapolles group (primitive angiosperms; 55–75%), while spores, gymnosperm pollen, and dinoflagellate cysts are less abundant. The Normapolles group is represented mainly by *Interporopollenites proporus*, *Longanulipollis longianulus*, *Plicapollis excelsus*, and the dinocysts by *Areoligera senonensis*, *Cerodinium diebelii*, *Dinogymnium acuminatum* and *Hystrichosphaeridium tubiferum*.

Meanwhile, a study of Late Campanian microfossils from the northern Eastern Carpathians by Bindiu et al. (2013) identified a foraminifera assemblage dominated by flysch-type agglutinated taxa as well as a low-to-moderate abundance of calcareous nannoplankton, suggesting bathyal environments, close to the calcite compensation depth. Maastrichtian assemblages of microfossils from the same area of the Eastern Carpathians contain different taxa of calcareous foraminifera such as *Abathomphalus mayaroensis*, *Globotruncana* div. sp., as well as common agglutinated foraminifera, such as *Caudammina ovula* and *Spiroplectammina spectabilis* (Ionesi, 1966; Ionesi and Tocorjescu, 1968).

Other integrated biostratigraphic studies (e.g., Țabără and Slimani, 2017; Țabără et al., 2017), focusing on upper Maastrichtian strata from the central-northern part of the Eastern Carpathians, allowed the identification of moderately diverse assemblages of dinocysts (e.g., *Cerodinium speciosum*, *Deflandrea galeata*, *Impagidium* sp., *Isabelidium cooksoniae*, *Pterodinium cretaceum*), calcareous nannoplankton (*Arkhangelskiella*

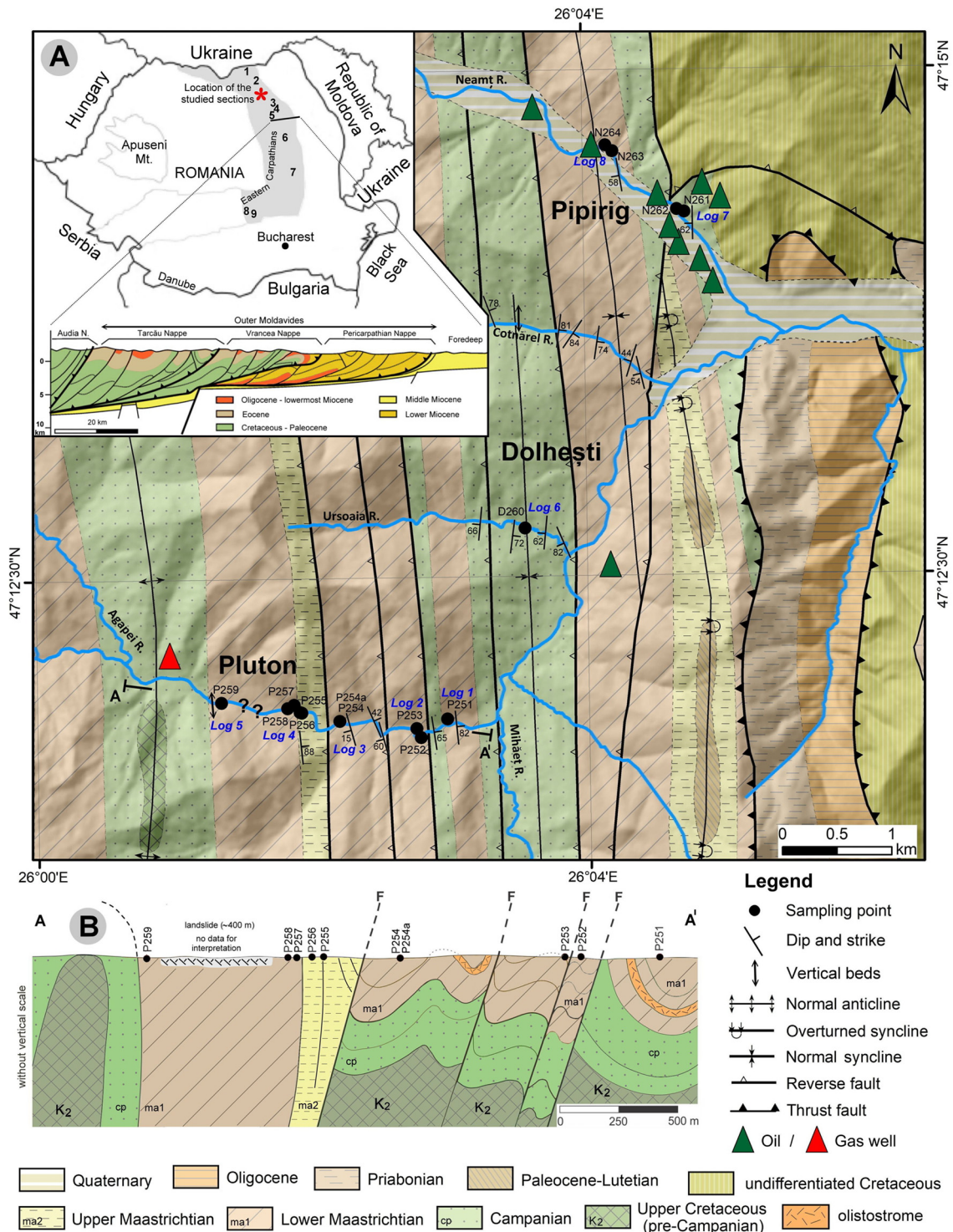


Fig. 1. A. The new geological map of the investigated area, with the location of the studied sections (Log 1 to Log 8). Some information, i.e., the location of the Bran-Dumesnic tectonic window (in the eastern part of the map), including the upper Eocene–Oligocene deposits assigned to the Vrancea Nappe, as well as the anticline fold on the western part of the area, were adapted from Piatra Neamț sheet (1:200,000 scale; Murgeanu and Mirăuță, 1968). A geological cross-section of the Eastern Carpathian Chain is also shown (after Leever et al., 2006). 1, 2, 3...8 inserted on the map of Romania represent the previous biostratigraphic studies: 1 - Bindiu et al. (2013; Suceava Valley), 2 - Ionesi and Todorjescu (1968), Antonescu and Alexandrescu (1979), Țabără et al. (2017) (Varnița Valley), 3 - Ion et al. (1982; Horăicioara Valley), 4 - Antonescu and Alexandrescu (1979), Ion et al. (1982), Țabără and Slimani (2017) (Cuejdiu Valley), 5 - Antonescu and Alexandrescu (1979; Oanțu Valley), 6 - Olaru (1978; Bistrița–Trotuș Valleys), 7 - Roban et al. (2017; Putna Valley), 8 - Cetean et al. (2011; Izlaz Valley), 9 - Melinte and Jipa (2005; Ialomița Valley); B. Geological cross-section along the Agapei River.

maastrichtiensis, *Micula prinsii*, *Nephrolithus frequens*, *Watznaueria barnesiae*), and foraminifera predominated by agglutinated forms (*Caudammina excelsa*, *Nothia excelsa*, *Placentammina placenta*). The palynofacies composition, marine phytoplankton assemblages, and

agglutinated foraminiferal morphogroups identified in these upper Maastrichtian deposits from the Hangu Formation, suggest an outer shelf to distal depositional environment for this interval. The Campanian–Maastrichtian red beds from the southern part of the Eastern

Carpathians reveal both cosmopolitan nannofossil assemblages as well as ones of Tethyan affinities (Melinte and Jipa, 2005; Bojar et al., 2009), allowing the assignment of the Moldavides Basin to the northern part of the Tethyan Realm.

4. Materials and methods

Eight stratigraphic sections (Log 1 to Log 8; Fig. 1A) from the upper part of the Hangu Formation were logged and sampled in the study area. Fourteen samples collected in these sections for palaeontological analysis have mostly yielded informative microfossil assemblages. It should be mentioned that all the analyzed samples come from various laminated black shales, lithologically similar, which suggests the same sedimentation conditions, therefore any kind of taphonomic modifications that could affect the microfossil assemblages can be considered to be roughly the same.

For the palynological and palynofacies analyses, all samples were processed using standard palynological techniques (e.g. Batten, 1999), involving HCl treatment to remove carbonates and HF treatment to remove the silicate minerals. Denser particles (mostly of mineral origin) were eliminated from the organic residue using $ZnCl_2$ with a density of 2.0 g/cm^3 . For this study, a kerogen oxidation procedure was not applied in order not to degrade delicate palynomorphs. The palynological residue was mounted on microscopic slides using glycerine jelly. Photomicrographs of palynomorph taxa (Plates I–IV, VIII–XI) were taken using a digital Leica DFC 420 camera mounted on a Leica DM1000 microscope. A complete palynofloral list, including dinoflagellate cysts, pollen and spores, is presented in Appendix A. The nomenclature of dinoflagellate taxa and references to their authors are based on the Dinoflag 3 database (Williams et al., 2017). All the microscopic slides are stored in the collection of the Geology Department, “Al. I. Cuza” University of Iași.

Marine palynomorphs usually consist of dinoflagellate cysts that are most common in neritic environments, and their abundance and diversity increase offshore, reaching a peak in outer neritic settings (Pross and Brinkhuis, 2005). Following earlier studies (e.g. Chakir et al., 2020; Maatouf et al., 2020; Biji et al., 2021; Niechwedowicz et al., 2021), the dinocyst assemblages are presented in eco-groups, according to their preferred niche on the continental shelf. One important palaeoenvironmental reconstruction approach used in this study is based on the relative abundances of selected dinocyst eco-groups, with significant palaeoecological indications, allowing the identification of nearshore shallow-water to oceanic open marine conditions. Changes in the composition, as well as in the abundance of the dinocyst eco-groups may be indicative of proximal–distal trends of the sedimentary basin (Sluijs et al., 2005; Maatouf et al., 2020). The following ratios, employed previously in palaeoenvironmental reconstructions (cf. Brinkhuis et al., 1998; Carvalho et al., 2016; Chakir et al., 2020) were also considered:

(1) the peridinioid to gonyaulacoid ratio (P/G), calculated by applying the eq. $P/G = nP/(nP + nG)$, where n is the number of dinocyst specimens counted, P – peridinioid dinocysts, and G – gonyaulacoid dinocysts. A peridinioid-dominated assemblage reflects low salinity and nutrient-rich conditions related to nearshore environments. By contrast, gonyaulacoid-dominated assemblages are indicators of open marine environments (Carvalho et al., 2013).

(2) the continental to marine palynomorphs ratio (C/M), also used as an indicator of a proximal–distal trend (Pellaton and Gorin, 2005; Ţabără et al., 2021). This ratio was calculated by applying the eq. $C/M = nC/(nC + nM)$, where n is the number of specimens counted, C – represents the sum of spore and pollen grains, and M – dinocysts. This ratio is used to estimate the terrestrial input (allochthonous components) into the marine basin. Generally, the C/M ratio decreases offshore.

Additional palaeoenvironmental information was also obtained based on palynofacies constituents (i.e. woody tissues, opaque phytoclasts, cuticles) recovered from samples. The high relative

abundance of often large woody material is often used to indicate proximal settings (Tyson, 1995; Aggarwal, 2022), whereas the high proportion of small-sized equidimensional opaque phytoclasts mainly suggests a distal depositional environment (Radmacher et al., 2020). The classification of the dispersed organic matter (kerogen) used in this study follows the guidelines of Ercegovac and Kostić (2006), Mendonça Filho et al. (2011), and Aggarwal (2022).

Nine samples (Appendix B) were selected for the analysis of foraminifera content. From these, 120 g were processed following standard micropaleontological methods (drying, weighing, soaking, boiling, and washing through a $63\ \mu\text{m}$ mesh sieve). Hardly dispersible samples were passed through two processing cycles and treated with hydrogen peroxide (H_2O_2) with a concentration of 3%. The dry residue from each sample was weighed before being analyzed using an Optika (SLX series) stereomicroscope. Foraminifera individuals were recovered from the $>63\ \mu\text{m}$ fraction and were preserved and classified in micropaleontological cells (stored in the collections of the Geology Department, Babeş-Bolyai University, Cluj-Napoca). Representative foraminifera (Plates V, VI) were photographed using a table top High Vacuum Scanning Electron Microscope with a Motorized StageV (EmCrafts CUBE 2) available at the Department of Geology, Babeş-Bolyai University. Other foraminifera specimens (Plate XII) were photographed in artificial light using an Optika SZM–1 stereomicroscope at the Geology Department of Babeş-Bolyai University. The identification of the foraminiferal taxa was based on representative papers concerning the Cretaceous of the Carpathian Neotethyan areas (e.g., Neagu et al., 1992; Kaminski and Gradstein, 2005; Cetean et al., 2011; Bindiu et al., 2013; Waškowska et al., 2020; Waškowska, 2021), and they are listed in Appendix B. Given that only a few of the analyzed samples (3 samples) provided a rich enough foraminifera content, multivariate statistical analyzes could not be performed.

In order to obtain palaeoenvironmental information, the foraminiferal counts were used to calculate abundance (i.e., the number of foraminifera individuals per gram of sediment), Fisher's alpha index (Fisher et al., 1943; Hammer and Harper, 2006), and percentages of agglutinated foraminifera morphogroups (Jones and Charnock, 1985; Kaminski and Gradstein, 2005; Cetean et al., 2011; Setoyama et al., 2011, 2017; Bindiu et al., 2013, 2016; Bindiu-Haitonic et al., 2019). Due to the tendency of tubular foraminifera to fragment, ten tubular fragments were considered to represent an individual. Samples that did not provide a sufficient number of agglutinated foraminifera (see Appendix B) were discarded from the palaeoenvironmental interpretations, whereas particularly good results were obtained from samples P255 and N261. The agglutinated foraminifera were used for palaeobathymetric reconstructions following the biofacies models proposed by Kaminski and Gradstein (2005).

Eleven samples (Appendix C) were prepared for calcareous nanoplankton analysis following the standard smear-slide technique (Blank and Young, 1998), and the resulting slides were examined using an Axiolab microscope with 1000 x magnification under plane- and cross-polarized light. At least 300 specimens per slide were counted whenever possible (with the notable exception of sample P256, with only 138 counted specimens), and another two longitudinal traverses were examined in order to specifically identify potential rarely occurring species. The calcareous nanoplankton species (Plates VII, XIII–XIV) were identified based on the online catalog Nannotax 3 (Young et al., 2017), and photographed using an AxioCam ERCS5 digital microscopy camera; the UC scheme of Burnett (1998) was employed for age assignment.

5. Results

5.1. New field observations

In our study of the Hangu Formation beds from the Pluton–Pipirig area, we analyzed eight local geological sections (i.e., Log 1 → Log 8;

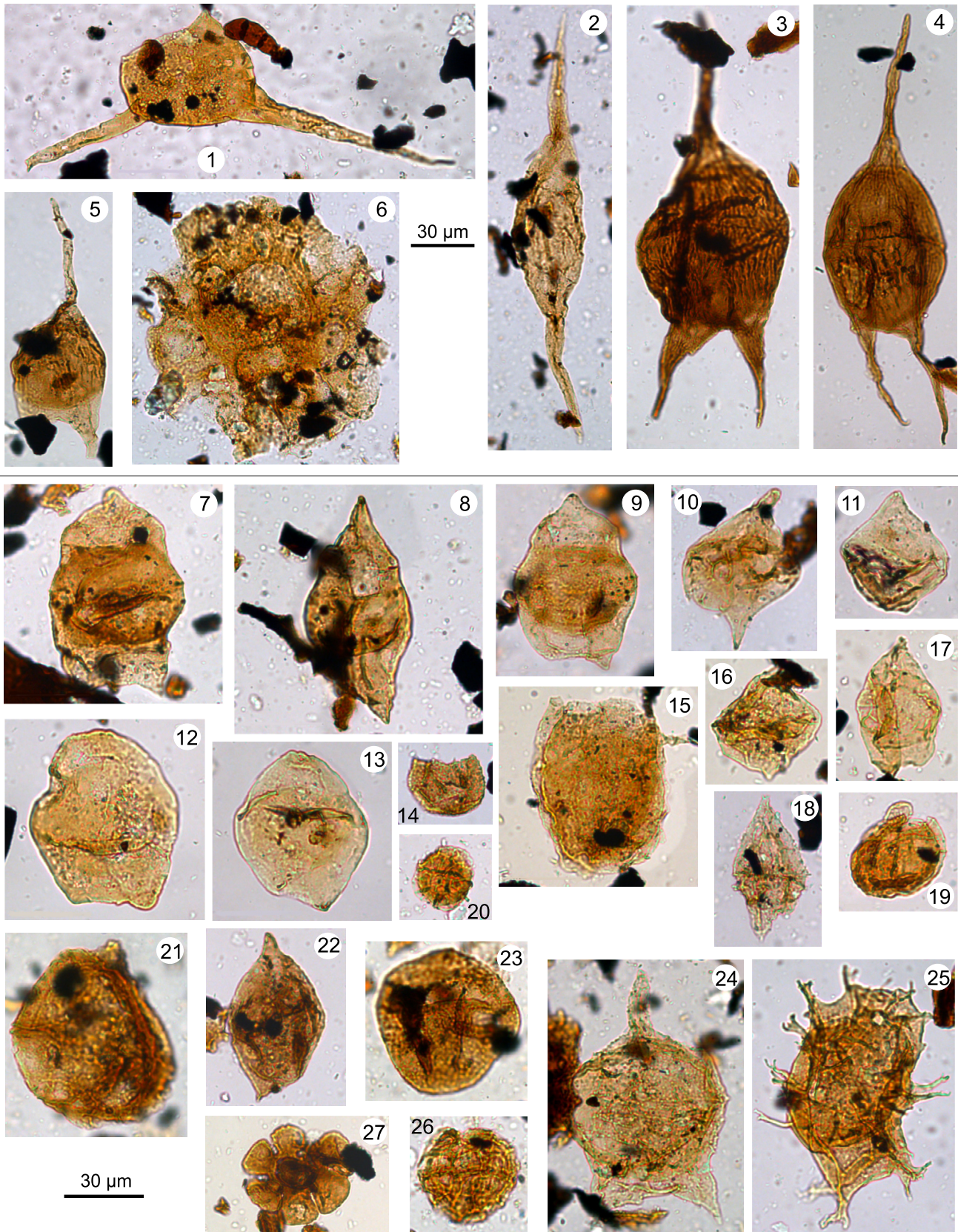


Plate I. Characteristic and stratigraphically important dinocysts from the upper Upper Campanian–Maastrichtian deposits of the Hangu Formation, Tarcău Nappe, Eastern Carpathians (the three numbers between brackets are related to samples, palynological slides and England Finder coordinates, respectively). 1. *Odontochitina operculata* (D260, TD/P347–2, C28). 2. *Palaeocystodinium golzowense* (P256, TD/P274–2, J39). 3. *Cerodinium striatum* (N264, TD/P278, O4). 4. *Cerodinium diebelii* (N264, TD/P278–1, B30). 5. *Cerodinium albertii* (P251, TD/P251–1, G33). 6. *Muratodinium fimbriatum* (P256, TD/P274, J37). 7. *Isabelidinium bakeri* (P258, TD/P252, M27). 8. *Isabelidinium microarmum* (P258, TD/P252, F13). 9. *Isabelidinium cooksoniae* (sample P256, TD/P274, B11). 10. *Alterbidinium acutulum* (P258, TD/P252–2, A25–2). 11. *Alterbidinium varium* (P254, TD/P255, D41). 12. *Isabelidinium weidichii* (N263, TD/P279–2, L29). 13. *Isabelidinium cretaceum* (N263, TD/P279–1, C23). 14. *Elytrocysta druggii* (P251, TD/P251–3, H33). 15. *Leberidocysta chlamydata* (P251, TD/P251–1, G10). 16. *Alterbidinium minus* (P254, TD/P255–3, G14). 17. *Isabelidinium acuminatum* (P254, TD/P255, L5–2). 18. *Alterbidinium montanaense* (D260, TD/P347–2, B19). 19. *Leberidocysta? microverrucosa* (P258, TD/P252–1, N38). 20. *Cladopyxidium paucireticulatum* (P258, TD/P252–1, H41–2). 21. *Cribroperidinium* sp. A of Brinkhuis & Schiøler (1996) (P256, TD/P274–2, G44). 22. *Manumiella? hemmoorensis* (P259, TD/P272–1, D33). 23. *Pierceites? chiengoviensis* (P256). 24. *Deflandrea galata* (P256, TD/P274–2, F8). 25. *Rottnestia wetzeli* subsp. *wetzeli* (N264, TD/P278–1, E38). 26. cf. *Microdinium sonciniae* (P256, TD/P274–1, J19–2). 27. Foraminifer test lining (P256, TD/P274–1, L34).

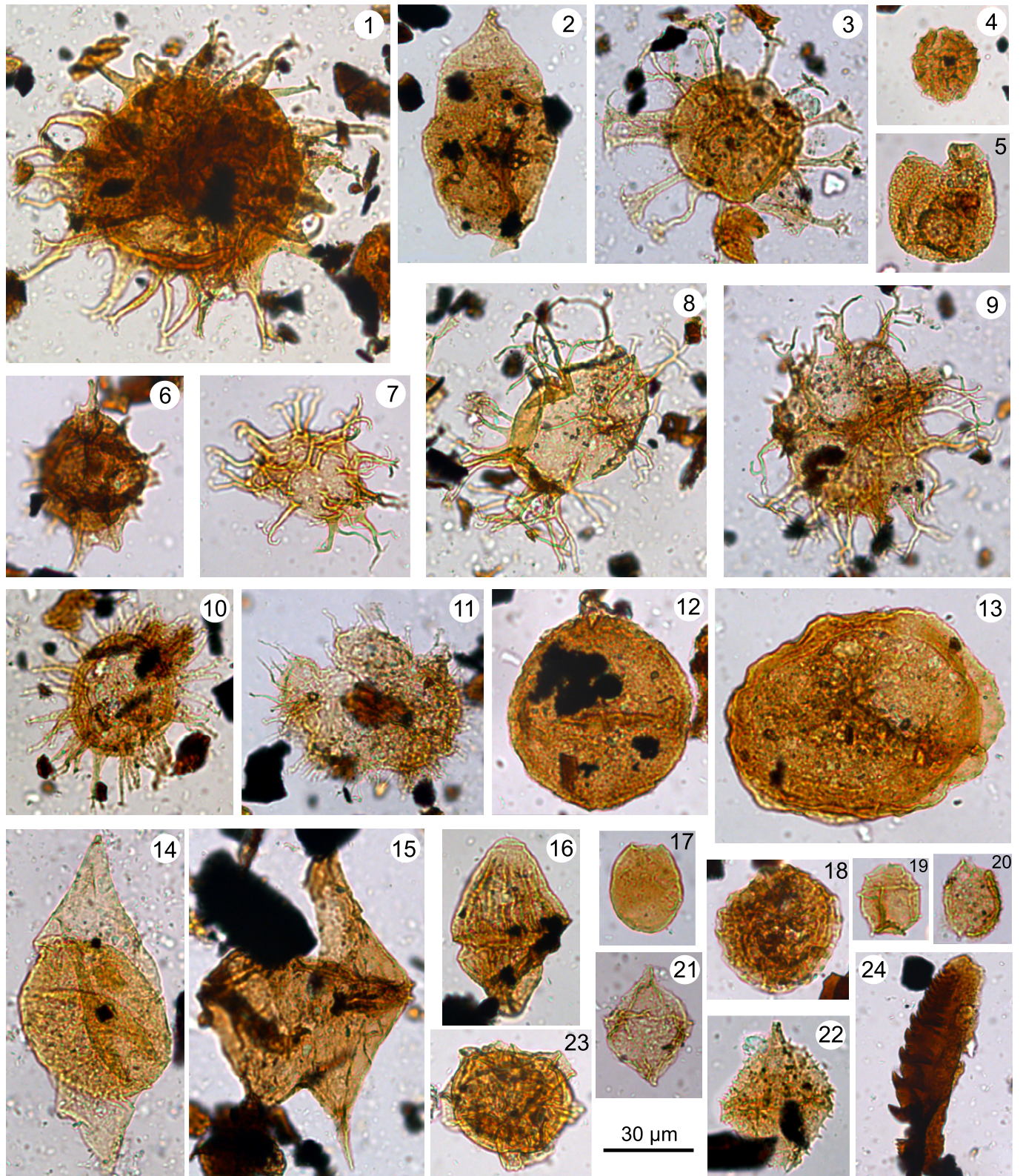


Plate II. Upper Upper Campanian–Maastrichtian dinocysts from the Hangu Formation, Tarcău Nappe, Eastern Carpathians (the three numbers between brackets are related to samples, palynological slides and England Finder coordinates, respectively). 1. *Fibrocysta axialis* (P256, TD/P274, D8). 2. *Chatangiella* sp. A of Schiøler and Wilson, 1993 (sample P251, TD/P251–2, C15). 3. *Hystriospheraidium tubiferum* subsp. *tubiferum* (P256, TD/P274–1, B25). 4. *Cladopyxidium paucireticulatum* (P259, TD/P272–3, D34). 5. *Batiacasphaera* sp. cf. *Batiacasphaera solida* (N263, TD/P279–2, D9). 6. *Spiniferella cornuta* subsp. *cornuta* (P259, TD/P272–3, G30–2). 7. *Surculosphaeridium longifurcatum* (N264, TD/P278–2, F22). 8. *Achomospaera ramulifera* (P256, TD/P274–2, E34). 9. *Spiniferites ramosus* (P256, TD/P274–1, F29–1). 10. *Pervospheraidium monasteriense* (P256, TD/P274, Y12). 11. *Impletosphaeridium clavulum* (P256, TD/P274–2, B22). 12. *Cassiculosphaeridia? intermedia* (D260, TD/P347–3, J44). 13. *Paralecaniella indentata* (N264, TD/P278–1, K23). 14. *Chatangiella? robusta* (N262, TD/P276–3, P22). 15. *Phelodinium tricuspis* (P256, TD/P274–1, C33). 16. *Dinogymnium acuminatum* (P253, TD/P342–2, L41). 17. *Fromea chytra* (N264, TD/P278–3, N30). 18. *Samlandia* cf. *mayi* (P253, TD/P342–4, F4). 19. *Phanerodinium? turnhoutensis* (N264, TD/P278, D41). 20. *Palaeostomocystis reticulata* (P252, TD/P340–2, A29). 21. *Diconodinium wilsonii* (D260, TD/P347, K17). 22. *Spinidinium echinoideum* (N264, TD/P278–1, C39). 23. *Pterodinium* sp. (N263, TD/P279–3, B44–1). 24. Scolecodont (reworked; D260, TD/P347–2, B28).

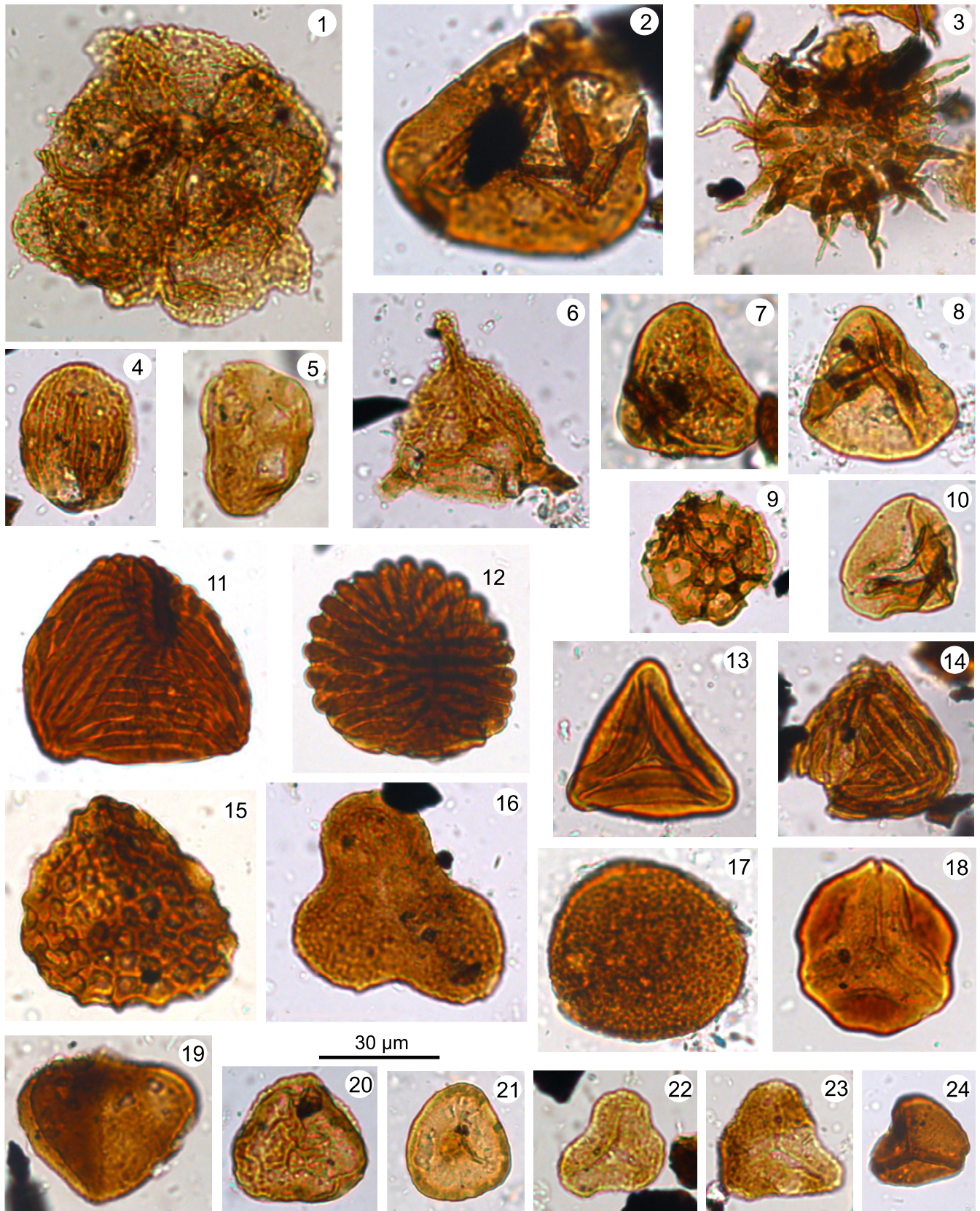


Plate III. Selected terrestrial palynomorphs (cryptogam spores) and other algae recovered from the Hangu Formation, Pluton-Pipirig area (the three numbers between brackets are related to samples, palynological slides and England Finder coordinates, respectively). 1 – algae; 2–24 – terrestrial palynomorphs. 1. *Palambage morulosa* (sample P254, TD/P255–3, D25). 2. *Deltoidospora australis* (D260, TD/P347–1, D37–2). 3. *Echinatisporis* sp. (P258, TD/P252, R13). 4. *Equisetosporites* sp. (P258, TD/P252, D2). 5. *Laevigatisporites haardti* (P254, TD/P255–3, K8). 6. *Appendicisporites* sp. (D260, TD/P347–2, F9). 7. *Deltoidospora punctatus* (N261, TD/P277–2, G40). 8. *Deltoidospora toralis* (N262, TD/P276, C22). 9. *Lycopodiumsporites* sp. (D260, TD/P347–2, C39). 10. *Deltoidospora minor* (N264, TD/P278, E11). 11. *Cicatricosisporites* sp. (N264, TD/P278–3, I10). 12. *Cicatricosisporites annulatus* (N263, TD/P279, B36). 13. *Gleicheniidites senonicus* (N262, TD/P276–3, G19–2). 14. *Cicatricosisporites spiralis* (D260, TD/P347–1, J34). 15. *Klukisporites pseudoreticulatus* (P254, TD/P255–1, E45). 16. *Concavissimisporites punctatus* (P252, TD/P340–2, I27). 17. *Vadaszisorites sacali* (N261, TD/P277, G18). 18. *Gleicheniidites latifolius* (P258, TD/P252–1, O33). 19. *Triplanosporites microsinosuosus* (P253, TD/P342–4, N19). 20. *Polypodiaceoisporites granulatus* (D260, TD/P347–2, E24). 21. *Stereisporites* sp. (N262, TD/P276–3, F23). 22. *Concavissimisporites* sp. (P254, TD/P255–2, C11). 23. *Deltoidospora* sp. (P254, TD/P255–3, D33). 24. *Biretisporites potoniaei* (P254, TD/P255–5, F33).

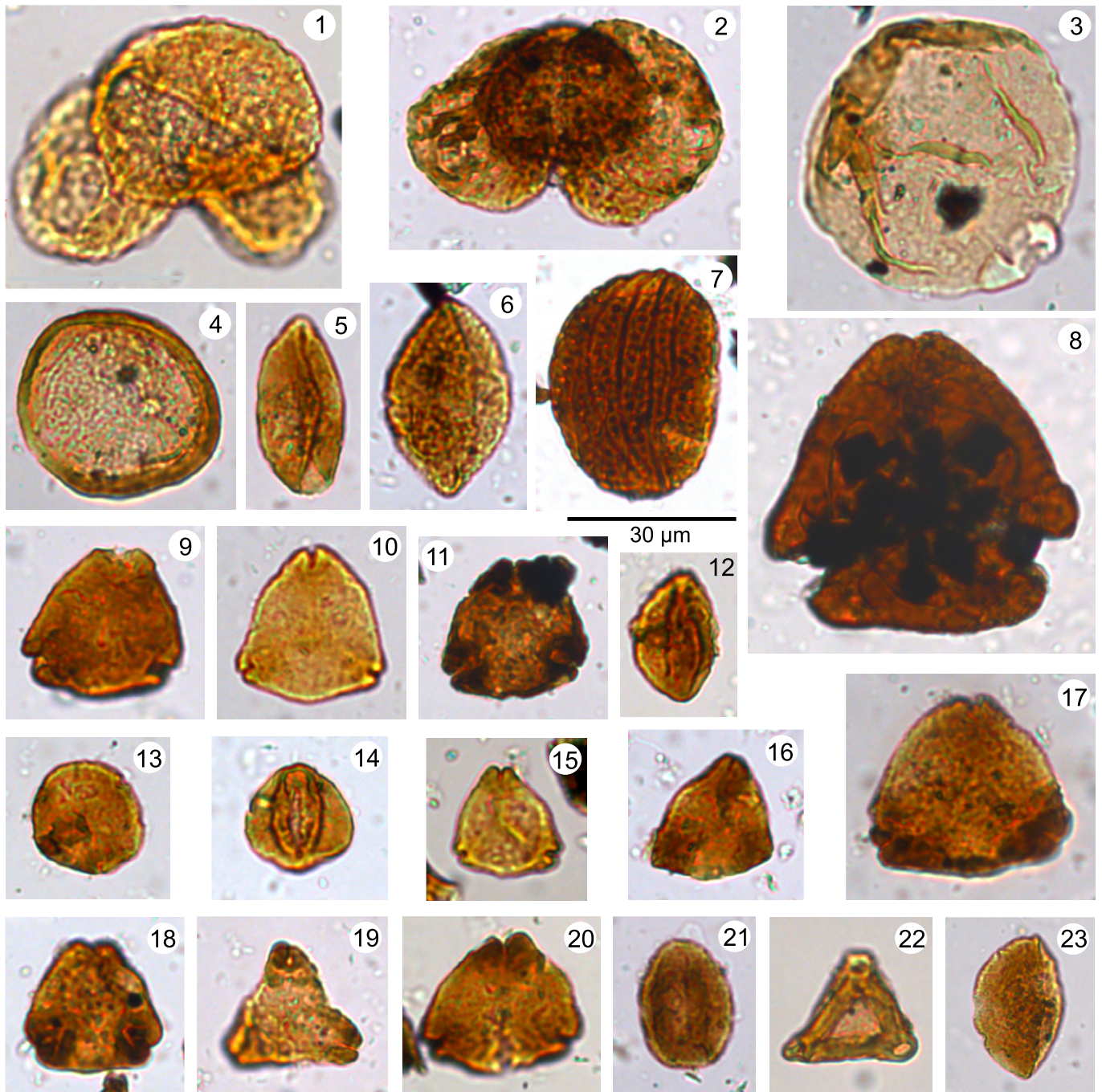


Plate IV. Selected gymnosperm and early angiosperm pollen grains recorded in the Hangu Formation, Pluton-Pipirig area (the three numbers between brackets are related to samples, palynological slides and England Finder coordinates, respectively). 1. *Pinuspollenites* sp. (sample P258, TD/P252-1, B28). 2. *Podocarpidites* sp. (D260, TD/P347-4, G37). 3. *Araucariacites australis* (N264, TD/P278-2, D34). 4. *Classopollis* sp. (N264, TD/P278-1, K39). 5. *Cycadopites follicularis* (D260, TD/P347-4, L11). 6. *Arecipites* sp. (P251, TD/P251, L32). 7. *Trisectoris* cf. *reticulatus* (D260, TD/P347-2, D2). 8. *Hungaropollis krutzschii* (N262, TD/P276-3, E25). 9. *Trudopollis nonperfectus* (D260, TD/P347-1, D3). 10. *Myricipites* sp. (N264, TD/P278-2, D44). 11. *Trudopollis spinulosus* (P259, TD/P272-2, N29). 12. *Tricolpites* sp. (P254, TD/P255-3, F25). 13. *Subtriporopollenites anulatus* (P251, TD/P251-2, A5). 14. *Cyrillaceapollenites* sp. (D260, TD/P347-3, I22). 15. *Myricipites bituitus* (P254, TD/P255-3, J19). 16. *Trudopollis baculotrudens* (P251, TD/P251-3, B4). 17. *Trudopollis acinosus* (D260, TD/P347-2, O27). 18. *Trudopollis minimus* (D260, TD/P347, F17). 19. *Vacuopollis venustus* (D260, TD/P347-3, M10). 20. *Plicapollis pseudoexelsus* (P252, TD/P340-2, I29-1). 21. *Bacutricolpites constrictus* (P252, TD/P340, L32). 22. *Interporopollenites proporus* (D260, TD/P347-2, D22). 23. *Monocolpopollenites* sp. (N263, TD/P279-2, F45).

Fig. 1A) located along the Neamț, Ursoaia and Agapei rivers, each one of these sections consisting of continuous sedimentary successions with thicknesses up to 40–45 m. According to our field observations, the deposits assigned to this geological unit are strongly folded into numerous syncline and anticline folds (Fig. 1B), as well as cross-cut by a complex fault system with N–S strike and westward dip (Fig. 1A). Lithologically, the analyzed sections include turbiditic deposits represented by

laminated black shales (5–80 cm thick), marlstones, and 10–50 cm thick calcarenite/sandstone interlayers. The top of Log 4 is made up of a succession composed mainly of calcarenites and sandstones that are rich in ichnofossils, and contain thin pelitic intercalations.

The deposits encountered on the Agapei River between Log 1 and Log 3 include a slumped body (8–10 m thick; Fig. 1B), consisting of a mixture of unstratified shales and sandstones, which can be considered

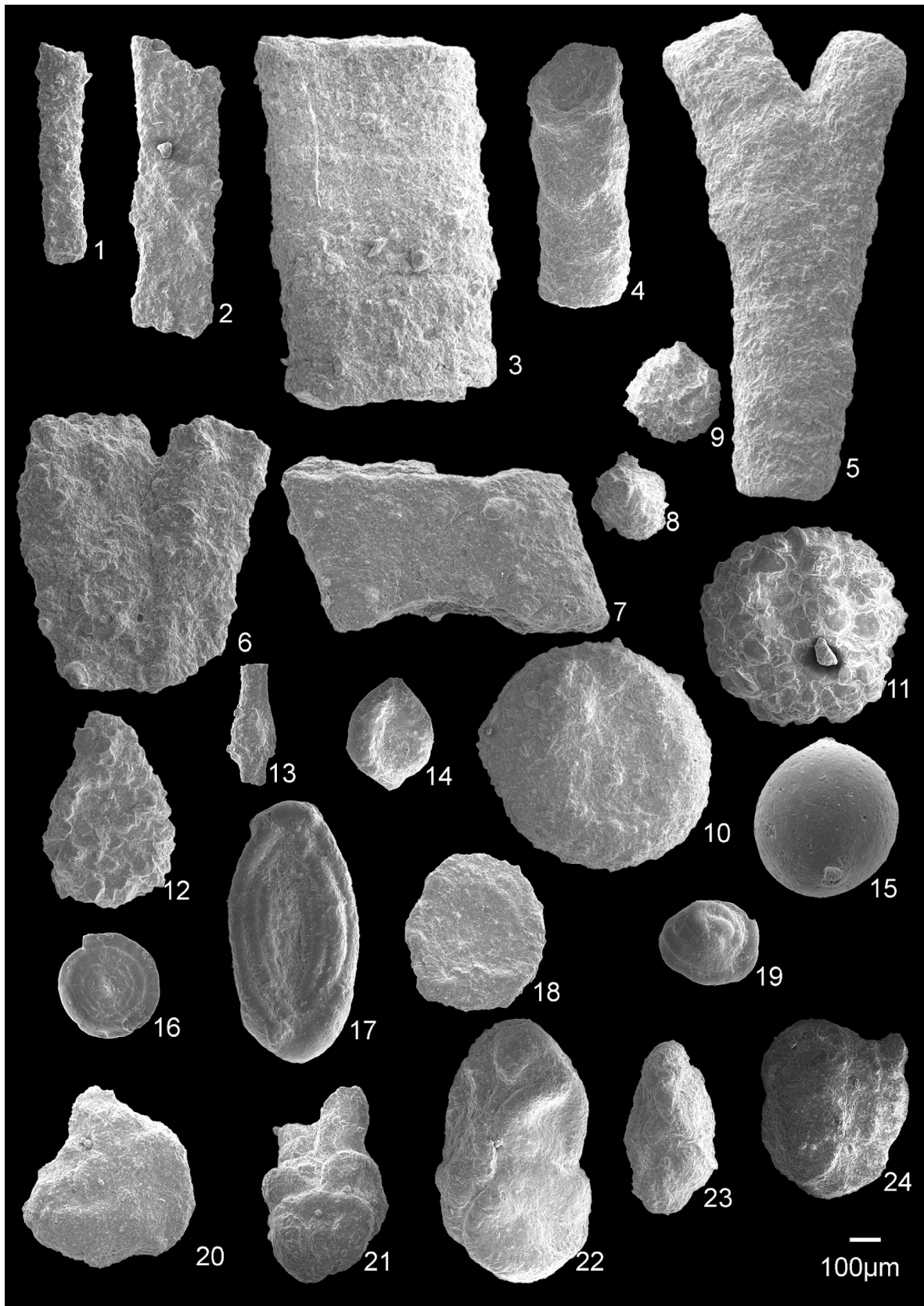


Plate V. Foraminifera assemblages from the from the Hangu Formation, Pluton-Pipirig area. 1. *Rhabdammina* sp. (sample P255). 2. *Rhabdammina* sp. (P255). 3. *Bathysiphon* (P256). 4. *Bathysiphon* sp. (N261). 5. *Nothia excelsa* (N261). 6. *Nothia excelsa* (P255). 7. *Nothia latissima* (P256). 8. *Saccammina grzybowskii* (P256). 9. *Saccammina grzybowskii* (P255). 10. *Psammosphaera irregularis* (N261). 11. *Psammosphaera irregularis* (P256). 12. *Hyperammina* sp. (P255). 13. *Caudammina excelsa* (P255). 14. *Caudammina ovulum* (P255). 15. *Caudammina gigantea* (P255). 16. *Ammodiscus cretaceus* (P255). 17. *Ammodiscus peruvianus* (P255). 18. *Ammodiscus* sp. (N261). 19. *Glomospira charoides* (P255). 20. *Lituotuba lituiformis* (N261). 21. *Paratrochamminoides* sp. (P255). 22, 23. *Trochamminoides subcoronatus* (P255). 24. *Trochamminoides variolarius* (sample P255).

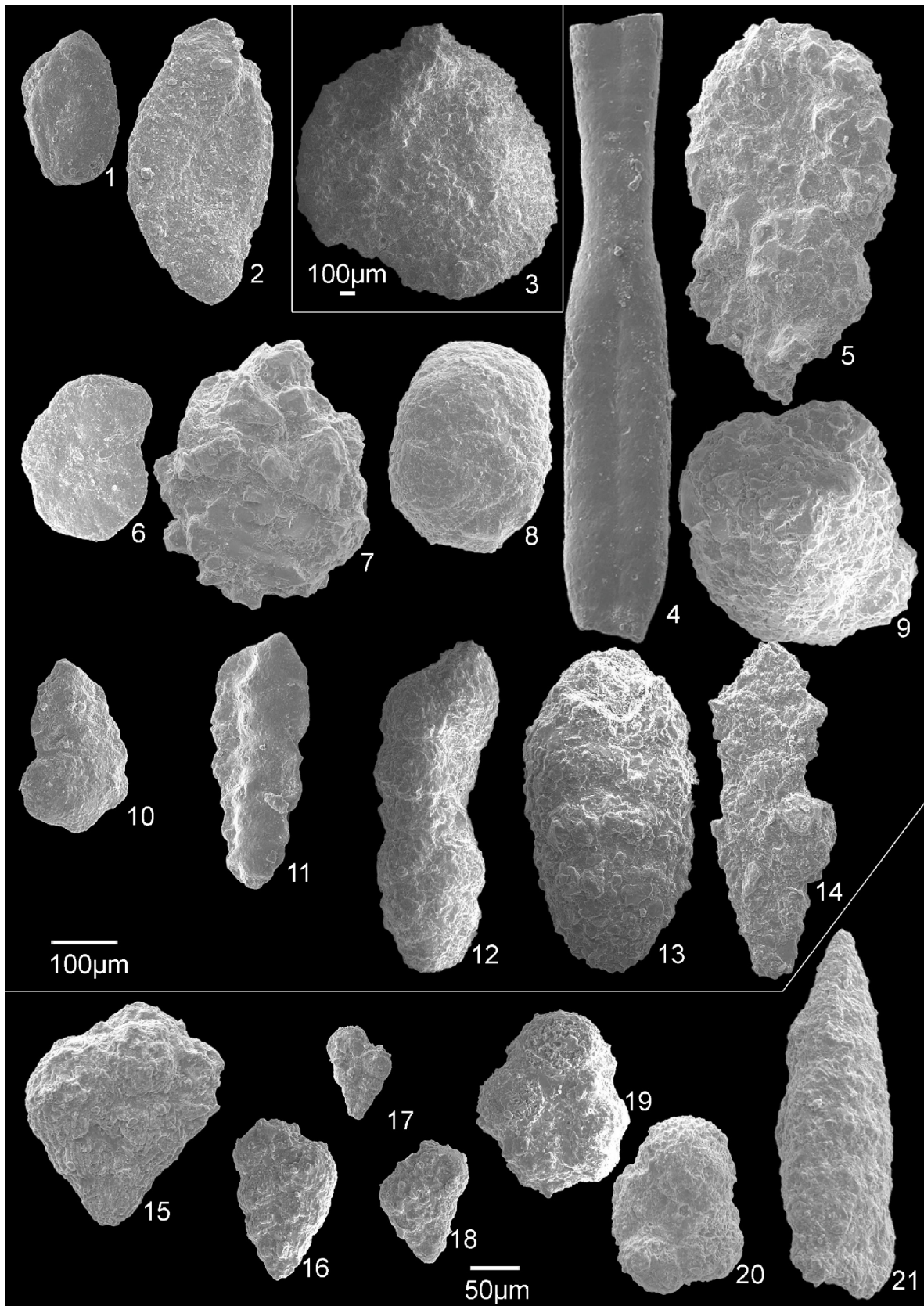


Plate VI. Foraminifera assemblages and radiolarians from the Hangu Formation, Pluton-Pipirig area. 1. *Rzehakina epigona* (P255). 2. *Rzehakina epigona* (N261). 3. *Aschemocella grandis* (P256). 4. *Kalamopsis grzybowskii* (P255). 5. *Hormosina* sp. (P255). 6. *Haplophragmoides* sp. (P255). 7. *Ammomarginulina* sp. (P255). 8. *Budashevaella multicamerata* (P255). 9. *Recurvoides* sp. (P255). 10. *Spiroplectammina spectabilis* (P255). 11. *Spiroplectammina* sp. (P255). 12. *Gerochammina lenis* (P255). 13. *Karrerulina* sp. (P255). 14. *Clavulina* sp. (N263). 15. *Planoglobulina* sp. (P251). 16. *Planoheterohelix planata* (P251). 17. *Planoheterohelix globulosa* (N264). 18. *Planoheterohelix* sp. (N264). 19. *Globigerinelloides* sp. (N263). 20. Reworked *Globigerinelloides* sp. (N263). 21. *Amphipyndax* sp. (Order Nassellaria, Radiolaria) (N261).

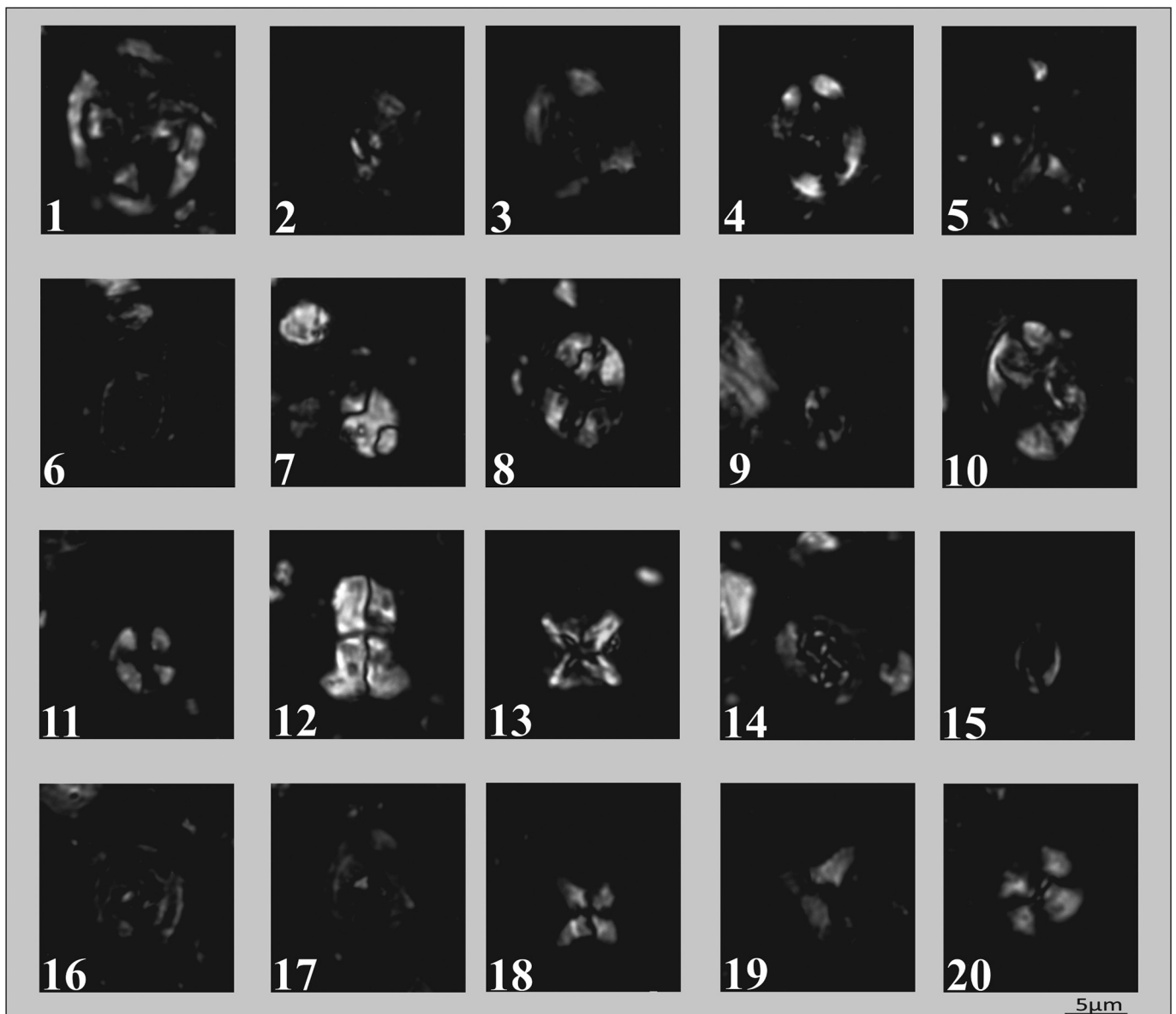


Plate VII. Selected calcareous nannoplankton from Hangu Formation. 1. *Arkhangelskiella cymbiformis* (sample P258). 2. *Biscutum constans* (P259). 3. *Broinsonia parca constricta* (P259). 4. *Broinsonia parca parca* (N262). 5. *Ceratolithoides aculeus* (P257). 6. *Cribrosphaerella ehrenbergii* (P257). 7. *Calculites obscurus* (P251). 8. *Eiffelithus eximius* (P255). 9. *Eiffelithus gorkae* (P257). 10. *Eiffelithus turrisieffellii* (P257). 11. *Eprolithus floralis* (N262). 12. *Lucianorhabdus maleformis* (P257). 13. *Micula staurophora* (P258). 14. *Prediscosphaera cretacea* (P255). 15. *Placozygus fibuliformis* (P256). 16. *Reinhardtites anthophorus* (P259). 17. *Reinhardtites levis* (P259). 18. *Uniplanarius sissinghii* (P257). 19. *Uniplanarius trifidus* (P259). 20. *Watznaueria barnesiae* (P257).

as an olistostrome deposited on the slope. Previously, olistostromes have also been described in the upper Maastrichtian–lower Paleocene deposits of the Vrancea Nappe (Tabără and Slimani, 2017).

5.2. Palynological content

The fourteen samples collected from the Hangu Formation of the Pluton-Pipirig area that were processed for these analyses yielded moderately rich palynological assemblages, consisting of both marine (17–95%) and terrestrial (5–83%) palynomorphs; two of these (P255 and P257) had a low palynomorph content. The microfloral assemblages consist of 167 identified taxa, including 88 dinocysts, 38 cryptogam spores, as well as 9 gymnosperm and 31 angiosperm pollen (Appendix A). Minor occurrences of bryophytes (1 taxon; Plate III, 21), foraminifera test linings (e.g., Plate I, 27), and reworked scolecodonts (Plate II, 24) have also been observed.

The peridinioid dinocysts (28 taxa) dominate the identified phytoplankton assemblage. These are mainly represented by *Alterbidinium acutulatum* (up to 16% in sample P253), *Alterbidinium varium*, *Cerodinium diebelii* (up to 15% in sample P251), *Chatangiella* div. sp., *Manumiella* div. sp., *Paleocystodinium golzowense*, all of which are shown to be biostratigraphically significant. Meanwhile, other peridinioid dinocysts that were also recorded in the studied samples are rare occurrences; these include *Cerodinium albertii*, *Cerodinium striatum*, *Diconodinium wilsonii*, *Isabelidinium acuminatum*, and *Laciniadinium firmum*. The gonyaulacoid dinocysts show a high diversity (46 taxa), including species such as *Achomosphaera ramulifera*, *Fibrocysta axialis*, *Hystrichosphaeridium tubiferum* subsp. *tubiferum*, *Leberidocysta* div. sp., *Pervosphaeridium monasteriense*, and *Spiniferites ramosus*, but individuals of this group are mainly common in Log 4 (sample P256) and Log 8 (sample N264). In addition, taxa assigned to dinogymnioid cysts (e.g., *Dinogymnium acuminatum*, *Dinogymnium longicorne*), as well as marine algae

(*Palambage morulosa*, *Pterospermella*), are less common elements in the assemblage.

The terrestrial palynomorph assemblage is dominated mainly by fern spores and angiosperm pollen, whereas the gymnosperms are less common. Fern spores, more specifically representatives of Cyatheales, Lycopodiaceae and Polypodiaceae, were frequently observed, with *Deltoidospora australis*, *Deltoidospora minor*, *Lycopodiumsporites* div. sp. and *Polypodiaceosporites* div. sp. as the most abundant species. Other commonly identified spore taxa include *Biretisporites potoniaei*, *Echinatisporis* sp., *Laevigatosporites haardti*, and *Triplanosporites microsinosus*. Angiosperm pollen are consistently recorded in all studied sections and are mostly represented by taxa assigned to the Normapolles group (e.g., *Hungaropollis krutzschii*, *Oculopollis praedicatus*, *Trudopollis nonperfectus*, *Trudopollis spinulosus*), Myricaceae (*Myricipites* div. sp.), and ancestral Juglandaceae (*Plicapollis pseudoexcelsus*, *Subtriporopollenites* spp.). A fairly similar assemblage of angiosperm pollen has been previously described from upper Campanian–Maastrichtian deposits located in the southwestern Transylvanian Basin (‡Tabără et al., 2022), the Hațeg Basin (‡Tabără and Slimani, 2019; Botfalvai et al., 2021), and the northern Moldavidian Domain (‡Tabără et al., 2017). The gymnosperm pollen show a low diversity, and are mainly represented by the Cheirolepidiaceae (*Classopollis* spp.), Pinaceae (*Pinuspollenites* spp., occurring with a slightly higher frequency in Log 7, sample N262), and Araucariaceae (*Araucariacites australis*). Other terrestrial palynomorphs such as peat mosses (*Stereisporites* sp.) represent a minor component of the assemblage.

5.3. Foraminiferal assemblages

Foraminifera species were identified in most investigated samples save two (samples P258 and N262) that were barren. Seventy foraminifera taxa were identified (Appendix B), among which the agglutinated foraminifera group is the best preserved and represented (with as many 55 species identified in sample P255), whereas the calcareous benthics and planktonics are poorly preserved, with 12 species and genera. Most of the agglutinated specimens are relatively large and have a coarse agglutinated test. The number of foraminifera per gram varies from log to log, and ranges from 5.97 (sample P259) to 67.84 (sample P255). Diversity was calculated only for sample P255 in which it registers a high value (Fisher's alpha index is 21.27). The benthic forms (agglutinated and calcareous benthic) dominate samples P255, P256, P259, and N261, whereas the benthic foraminifera are exceeded by the planktonic forms in the remaining samples (P251, N263, and N264). Except for the M3b morphotype (flattened irregular: *Ammolagena clavata*; Kaminski and Gradstein, 2005), all the other morphogroups are represented in the studied samples. A relatively balanced distribution of the morphogroups was observed in sample P255; the highest percentages in this sample are recorded by the morphogroups M2b (rounded streptospiral: *Recurvoides* spp.) and M4b (elongate subcylindrical and tapered: *Hormosina velascoensis*, *Gerochammina lenis*, *Karrerulina conversa*, *Karrerulina horrida*, *Subreophax scalaris*), followed in order of decreasing percentage by the morphotypes M3a (flattened planispiral and streptospiral: *Ammodiscus cretaceus*, *Ammodiscus peruvianus*, *Glomospira charoides*, *Rzehakina epigona*, *Rzehakina* sp.), M3c (flattened streptospiral: *Ammosphaeroidina pseudopauciloculata*, *Paratrochamminoides* spp., *Trochamminoides subcoronatus*), M1 (tubular: *Bathysiphon* sp., *Nothia excelsa*, *Nothia latissima*, *Rhizammina* sp., *Kalamopsis grzybowskii*), M2a (globular: *Saccammina grzybowskii*, *Psammosphaera irregularis*, *Aschemocella grandis*, *Caudammina gigantea*, *Caudammina excelsa*), M2c (elongate keeled: *Spiroplectammina spectabilis*), and M4a (rounded planispiral: *Haplophragmoides* sp.). Although the number of tubular fragments (M1 morphogroup) was divided by 10 to arrive to an estimated individual count, these forms – *Bathysiphon* sp., *Rhizammina* sp., *Rhabdammina* sp., and *Nothia* spp. – consistently dominate in sample N261 (up to 84% of the assemblage). In the same sample, very low percentages (below 7%) of morphotypes M2b (*Recurvoides* sp.), M3a

(*Ammodiscus* sp. and *Rzehakina* sp.), and M3c (*Paratrochamminoides* sp.) can also be noted.

5.4. Calcareous nannoplakton

The calcareous nannoplankton assemblages recovered from the Hangu Formation deposits of the Pluton-Pipirig area consist of 60 species (Plates VII, XIII–XIV; Appendix C), characterized by moderate degree of preservation and moderate abundance. The dominant species in the assemblage is *Micula staurophora* (up to 66.33% in sample P251, with a mean of 46.84%), followed in terms of abundance by *Watznaueria barnesiae* (up to 28.70% in sample P259, with a mean of 18.97%), *Arkhangelskiella cymbiformis* (up to 30.29% in sample P258, with a mean of 7.98%), *Lucianorhabdus maleformis* (up to 7.66% in sample P251, with a mean of 3.82%), and *Prediscosphaera cretacea* (up to 5.88% in sample P254, with a mean of 3.69%). Taxa occurring with low frequencies include *Biscutum coronum*, *Braarudosphaera bigelowii*, *Ceratolithoides aculeus*, *Chiastozygus litterarius*, *Gorkaea pseudanthophorus*, *Misceomarginatus pleniporus*, and *Uniplanarius trifidus*.

Overall, the deposits assigned to the Campanian–Maastrichtian transition and the lower Maastrichtian include most of the nannofossil species, but some of taxa (i.e. *Chiastozygus amphipons*, *Micula premolisilvae*, *Rhagodiscus splendens* and *Staurolithites laffittei*) occur only in the younger, upper Maastrichtian deposits of the studied sections.

5.5. Palynofacies compositions

In the studied sections the dispersed organic matter, as observed under the microscope, is moderately well preserved and mainly composed of kerogen of terrestrial origin. Four main palynofacies components were recognized in the samples, including: translucent phytoclasts (woody tissues derived from higher plants, cuticles, and membranes), opaque phytoclasts (equidimensional and less lath-shaped), palynomorphs (of marine and terrestrial origin), and a minor fraction of gelified amorphous organic matter (of continental origin). In addition, the palynofacies also include small amounts of granular amorphous organic matter (from marine sources), rare foraminifer test linings, and reworked scolecodonts.

Palynofacies assemblages recovered from most of the samples from the logged sections 2, 5, 6, 7, and 8 are dominated by translucent phytoclasts (up to 65% in sample P252) sometimes of large size, complemented by both equidimensional and lath-shaped opaque phytoclasts. According to the classification of Ercegovac and Kostić (2006), the kerogen macerals recovered from the sections listed above are represented by vitrinite (brown translucent phytoclasts), cutinite (yellow translucent phytoclasts), inertinite (opaque phytoclasts), and liptinite (including spores and pollen grains, and phytoplankton). The palynomorphs encountered are of both marine and terrestrial origins; they appear with low frequencies (1–3%) and show C/M ratios ranging between 0.34 and 0.9.

A slight change in palynofacies composition is recorded in three sections located along the Agapei River (i.e., logs 1, 3, and 4), containing slightly younger deposits compared to those described in the sections discussed previously. In these three sections, the proportion of opaque phytoclasts frequently exceeds 70% of the total kerogen, reaching 95% in sample P255 from Log 4. They most often are small and sometimes have a rounded shape as a result of prolonged transport. Such “allochthonous” fraction of organic particles can be distributed in the marine basin far from its original terrestrial source area (Tyson, 1995). In the upper part of the Log 4 section (i.e., in sample P256), the composition of kerogen consisting mainly of opaque phytoclasts, coincides with a high proportion of gonyaulacoid cysts, reflecting outer neritic-oceanic conditions. In the same sample, both the P/G and the C/M ratios are low, amounting to only 0.34 and 0.04, respectively.

6. Discussion

6.1. Biostratigraphy

The dinocysts, as well as the calcareous nannoplankton and foraminiferal assemblages recovered from the studied samples were useful in establishing a comprehensive biostratigraphic framework for the eight analyzed sections of the Hangu Formation in the Pluton-Pipirig area. Of these three groups of microfossils, better-constrained age assessments were provided by important dinocyst marker taxa (see below). Meanwhile, certain calcareous nannoplakton taxa that are frequently used for biostratigraphic assessments of Upper Cretaceous deposits have a wider range between the Campanian and the early (or even late) Maastrichtian, being thus less well suited for accurate age assignments. Furthermore, it is likely that some of the marker nannoplankton species were reworked in some of the analyzed samples, as these indicate a slightly older age than that provided by the dinocyst assemblages.

Most of the identified planktonic foraminifera show an extremely poor degree of preservation (see Plate VI), and the few taxa that could still be identified at the species level are unreliable markers due to their relatively extensive stratigraphic ranges, and are thus largely useless for detailed biostratigraphical interpretations. Meanwhile, the agglutinated foraminifera form a well-represented group in deep-water deposits (both above and below the calcite compensation depth), due to their durable tests; even though many agglutinated taxa also have relatively extensive stratigraphic ranges, their interval zones, partial range zones, or particular acmes were successfully used in biostratigraphic studies at least for the Upper Cretaceous deposits of the Carpathians (e.g., Bratu, 1965; Ionesi and Tocorjescu, 1968; Morgiel and Olszewska, 1981; Geroch and Nowak, 1984; Neagu, 1990; Neagu et al., 1992; Olszewska, 1997; Bąk, 2000; Malata, 2002; Oszczypko et al., 2005; Cetean et al., 2011; Țabără et al., 2017; Bindu et al., 2013, 2016; Bindu-Haitonic, 2018; Bindu-Haitonic et al., 2017, 2019; Waškowska-Oliwa, 2003, 2005, 2008; Waškowska et al., 2020; Waškowska, 2021). In the present study, only sample P255 (from Log 4) provided a rich and well-preserved assemblage of agglutinated foraminifera which, in addition to the palaeoenvironmental information it provides, also allowed a wider biostratigraphic framing of the hosting deposits.

Therefore, the more accurate biostratigraphic interpretations of the studied sections are based mainly on comparisons with well-calibrated Campanian–Maastrichtian dinocyst assemblages described from areas of relevant global stratotypes as well as from other regions. These include several important sections located in western Europe, particularly the GSSP for the base of the Maastrichtian at Tercis les Bains in France (Antonescu et al., 2001a, 2001b; Schiøler and Wilson, 2001), in the Maastrichtian type area in Belgium and the Netherlands (Slimani, 2000, 2001, recently recalibrated in Vellekoop et al., 2022), and Spain (Radmacher et al., 2014), as well as in eastern Europe in Poland (Slimani et al., 2021a; Niechwedowicz and Walaszczyk, 2022), in Romania (Antonescu and Alexandrescu, 1979; Țabără and Slimani, 2017; Țabără et al., 2017), and in southwest Crimea (Baraboshkin et al., 2020). Besides these, dinocyst biostratigraphy studies from the Mediterranean region, e.g., from Morocco (Slimani et al., 2010, 2016, 2021b; Jbari et al., 2020), as well as from elsewhere (Williams et al., 2004), were also very useful.

We have dated the eight studied sections based mainly on first occurrences (FOs) and last occurrences (LOs) of selected dinocyst species, but also of other identified microfossils (calcareous nannoplankton, foraminifera), whose stratigraphic distributions are shown in Fig. 2. According to our newly acquired and synthesized data, in the studied stratigraphic interval of the Hangu Formation from the Pluton-Pipirig area, previously dated loosely as Late Cretaceous–Paleocene (see Murgeanu and Mirăuță, 1968), the age of the deposits can be restricted to the late Late Campanian–early late Maastrichtian time interval as follows:

6.1.1. Late Campanian

The sample D260 collected from Log 6 is here dated as late Late Campanian, based on the following dinocyst bioevents: the FOs of *Alterbidinium montanaense* (Plate I, 18), *Cassiculosphaeridia? intermedia* (Plate II, 12), and *Diconodinium wilsonii* (Plate II, 21) which are indicative of the late Late Campanian in many areas (Slimani, 2000, 2001; Jbari et al., 2020; Slimani et al., 2021a), as well as the LO of *Odontochitina operculata* (Plate I, 1) which is no younger than latest Campanian (Williams et al., 2004; Slimani et al., 2021a, 2021b; Niechwedowicz, 2019). This sample also contains a taxon of Normapolles pollen, i.e., *Trudopollis acinosus* (Plate IV, 17), that is known to range from the Santonian to the Campanian (Polette and Batten, 2017).

A slightly younger age, close to the Campanian–Maastrichtian boundary, is revealed by the palynological assemblages identified in the N261–N262 sampling interval (Log 7; Fig. 2). These include *Chatagiella? robusta* (Plate II, 14), the LO of which is a typical marker of the Campanian–Maastrichtian boundary transition (Schiøler and Wilson, 2001), or is frequently quoted from Upper Campanian beds from Austria (Mohamed and Wagreich, 2013), the Meer borehole (Slimani et al., 2011), the Turnhout borehole (Slimani, 2000, 2001), and Morocco (Jbari et al., 2020; Slimani et al., 2021b). Its LO is reported to occur in the early Maastrichtian (May, 1980; Firth, 1987; Aurisano, 1989).

Two terrestrial palynomorph taxa with biostratigraphic significance, i.e., *Hungaropollis krutzschii* (Plate IV, 8) and *Vadaszsporites sacali* (Plate III, 17), also occur in samples N262 and N261, respectively. According to Polette and Batten (2017), *Hungaropollis krutzschii* occurs in the upper Santonian–Campanian interval from central Europe, while *Vadaszsporites sacali* which derives from a typical Early Cretaceous fern, may have persisted up to the Campanian in Hungary (Góczán and Siegl-Farkas, 1990), as well as in the Hațeg Basin (Țabără and Slimani, 2019) and the southwestern of the Transylvanian Basin (Țabără et al., 2022) in western Romania. The palynological assemblage recovered from sample N261 also includes several specimens of pollen derived from ancestral Juglandaceae (i.e., *Subtriporopollenites* div. sp.), a floral element that seems to have gradually replaced Normapolles-producing plants during the Late Campanian (Peyrot et al., 2020). This replacement of the Normapolles group with their modern counterparts (various Juglandaceae) was also recorded in the upper Upper Campanian from the southwestern Transylvanian Basin (Țabără et al., 2022).

According to UC zones introduced by Burnett (1998), the calcareous nannoplankton assemblage recovered from the N261–N262 sampling interval contains marker species with the FOs within the Campanian and their LOs within the Campanian or Maastrichtian. Three such marker species are present in this sampling interval, namely: i) *Broinsonia parca parca* (Plate VII, 4) with the LO within the UC15d biozone (Campanian; Burnett, 1998); ii) *Broinsonia parca constricta* (Plate VII, 3) with the LO within the UC16 zone (early Maastrichtian; Burnett, 1998); and iii) *Uniplanarius sissinghii* (Plate VII, 18) with the LO in the early Maastrichtian (Burnett, 1998). Four other taxa of this assemblage (i.e., *Gorkaea pseudanthophorus*, *Micula clypeata*, *Misceomarginatus pleniporus* and *Reinhardtites levis*) are also restricted to the Campanian–Maastrichtian (Burnett, 1998; Young et al., 2017).

Furthermore, even if the foraminifera species *Rzehakina epigona* (Plate VI, 2) was identified only in very small numbers in sample N261, its presence in the assemblage also supports the previous age assessment, as this taxon had been reported from the Eastern Carpathians by Neagu (1990) as having its FO in the upper part of the Upper Campanian.

6.1.2. Early Maastrichtian–earliest late Maastrichtian

Most of the studied sections, i.e., Log 1, Log 2, Log 3, the lower part of Log 4, Log 5, and Log 8 (Fig. 2), contain deposits assigned here to the early Maastrichtian–earliest late Maastrichtian time interval. This age assignment is based on the FOs of *Alterbidinium varium* (Plate I, 11), *Cladopyxidium paucireticulatum* (Plate I, 20; Plate II, 4), *Isabelidinium*

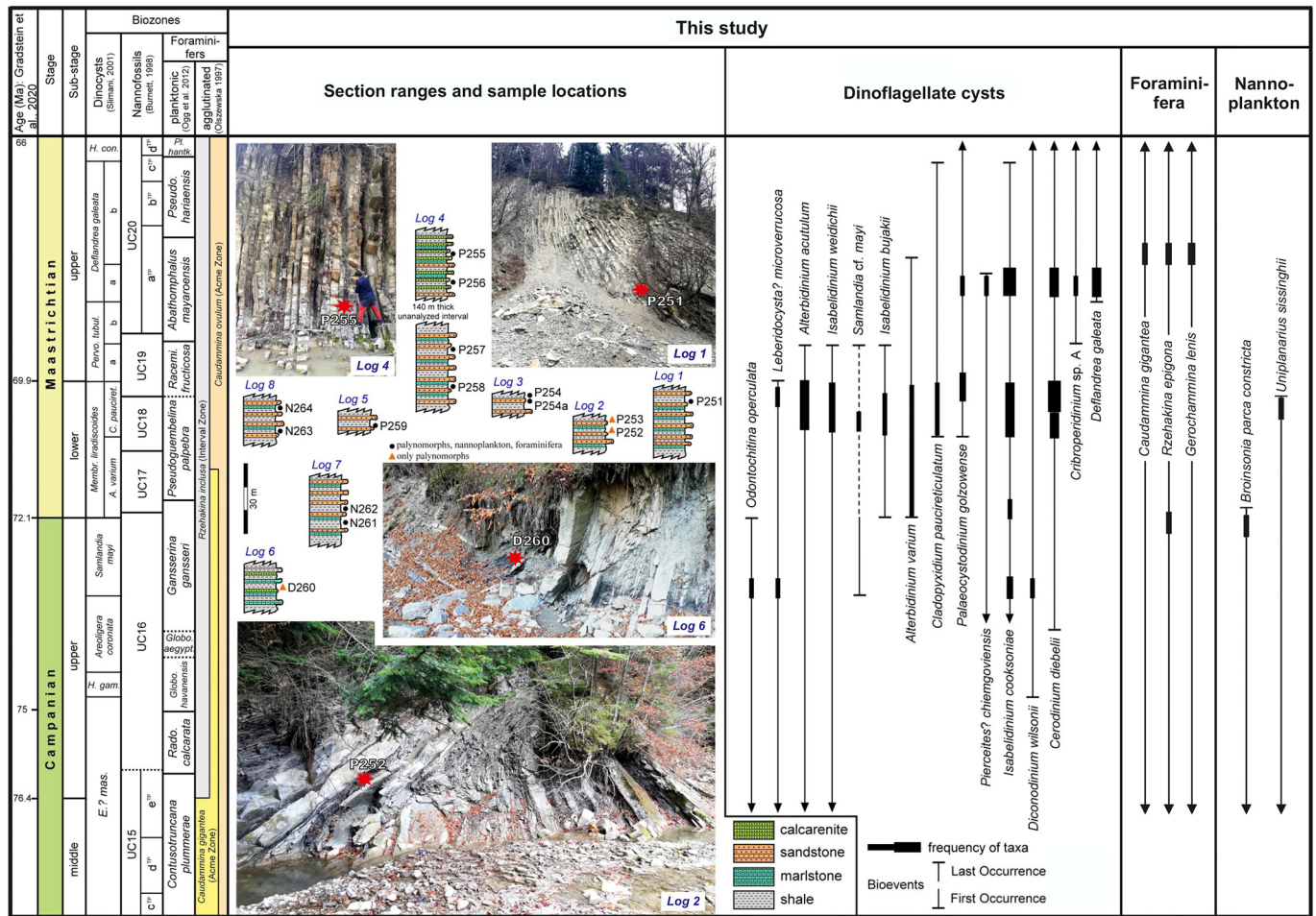


Fig. 2. Stratigraphy of the Pluton–Pipirig composite sections, showing the ranges of the sections studied and sample locations. Stratigraphic distribution of selected microfossils and bioevents are also shown. Dinocyst zonation after Slimani (2001), recently recalibrated in Vellekoop et al. (2022); calcareous nannoplankton zonation, UC zones after Burnett (1998); planktonic foraminiferal zonation after Ogg et al. (2012) and agglutinated foraminiferal zones according to Olszewska (1997). Abbreviations: *E.? mas.* = *Exochosphaeridium? masureae*; *H. gam* = *Hystrichokolpoma gasospina*; *Membr. liradiscoides* = *Membranilarnacia liradiscoides*; *A. varium* = *Alterbidinium varium*; *C. pauciret.* = *Cladopyxidium paucireticulatum*; *Pervo. tubul.* = *Pervosphaeridium tubuloaculeatum*; *H. con.* = *Hystrichostrogylon coninckii*; *Rado. calcarata* = *Radotruncana calcarata*; *Globo. havanensis* = *Globotruncanella havanensis*; *Globo. aegypt.* = *Globotruncana aegyptiaca*; *Racemi. fructiosa* = *Racemiguembelina fructiosa*; *Pseudo. hariaensis* = *Pseudoguembelina hariaensis*; *Pl. hantk.* = *Plummerita hantkeninoides*.

cf. *bujakii* (Plate VIII, 13) and *Palaeocystodinium golzowense* (Plate I, 2), and, respectively, the LOs of *Alterbidinium acutulum* (Plate I, 10), *Isabelidinium weidichii* (Plate I, 12), *Leberidocysta? microverrucosa* (Plate I, 19), and *Samlandia cf. mayi* (Plate II, 18).

The most common biostratigraphic marker encountered in the sections listed above is *Alterbidinium varium*. Its FO marks the Late Campanian in the Mediterranean area and in southern Europe (Eshet et al., 1994; Antonescu et al., 2001a, 2001b; Schiøler and Wilson, 2001; Jbari et al., 2020; Slimani et al., 2021b), but is slightly younger (Campanian–Maastrichtian boundary) in northern Europe (Kirsch, 1991; Slimani, 2000, 2001; Baraboshkin et al., 2020). The FO of *Isabelidinium bujakii* was also recorded within the lower Maastrichtian in Germany (Marheinecke, 1986), and simultaneously with the FO of *Alterbidinium varium* at the Campanian–Maastrichtian boundary and at the base of the dinocyst *Membranilarnacia liradiscoides* Zone (base of the *Alterbidinium varium* Subzone) (Slimani, 1995, 2000, 2001) in the Maastricht area. *Alterbidinium varium* and *Isabelidinium cf. bujakii* first occur simultaneously in Log 8, in sample N263 (Fig. 2). The FOs of *Cladopyxidium paucireticulatum* and *Palaeocystodinium golzowense* were recorded slightly higher in the lower Maastrichtian, within the *Membranilarnacia liradiscoides* Zone (base of the *Cladopyxidium paucireticulatum* Subzone) (Slimani, 1995, 2000, 2001). These two taxa first occur in Log 1 (sample P251), as well as in the lower parts of section logs 2 (sample P252), 4 (sample P258), 5 (sample P259), and

8 (sample N263) (Fig. 2), supporting an age not older than the middle part of the early Maastrichtian for these sections.

Cerodinium diebelii (Plate I, 4), whose FO is a worldwide marker of the Late Campanian (Antonescu et al., 2001a, 2001b; Slimani, 2001; Radmacher et al., 2014), is recorded with different frequencies only from the Maastrichtian deposits of the study area. According to Baraboshkin et al. (2020), a peak of abundance of *Cerodinium diebelii* was reported from the lowermost Maastrichtian of the Beshkosh section (Crimea). This bioevent is observed in slightly younger deposits of the Eastern Carpathians, assigned here to the upper part of the lower Maastrichtian (Fig. 2).

The LOs of *Alterbidinium acutulum*, *Isabelidinium bujakii*, *I. weidichii* and *Samlandia cf. mayi* are very good markers of the early Maastrichtian (Kirsch, 1991; Schiøler and Wilson, 1993; Slimani, 2000, 2001; Antonescu et al., 2001b; Baraboshkin et al., 2020; Jbari et al., 2020; Slimani et al., 2021a). However, recently, these bioevents were shown to suggest an earliest late Maastrichtian age, according to the upper Cretaceous dinocyst zones of Slimani (2001) recalibrated in Vellekoop et al. (2022). Therefore, the deposits of logged sections 1, 2, 3, 4 (its lower part), 5, and 8 cannot be younger than the earliest late Maastrichtian.

The calcareous nannoplankton assemblages identified in Log 3, in the lower part of Log 4, and in Log 5, also contain Campanian–early Maastrichtian marker taxa such as *Broinsonia parca parca* (Plate VII, 4), *Broinsonia parca constricta* (Plate VII, 3), *Ceratolithoides aculeus* (Plate

VII, 5), *Uniplanarius sissinghii* (Plate VII, 18), and *Uniplanarius trifidus* (Plate VII, 19). In association with these taxa, other typical Campanian–Maastrichtian species (e.g., *Micula clypeata*, *Micula premolisilvae*, *Prediscosphaera stoveri*, and *Reinhardtites levis*) were also recorded as part of the calcareous nannoplankton assemblages. Accordingly, within these nannofossil assemblages, the occurrences of taxa such as *Broinsonia parca parca*, whose LO marks the UC15d biozone (middle Campanian) in Maastrichtian deposits of Log 4 could suggest the action of reworking processes, as was previously recognized for calcareous nannoplankton in other sites (Machaniec et al., 2020; Mahanipour et al., 2022).

The nannoplankton assemblages of samples P251 (Log 1), as well as N263 and N264 (Log 8), are mainly represented by long-ranging taxa such as *Arkhangelskiella cymbiformis* (Plate VII, 1), *Calculites obscurus* (Plate VII, 7), *Lucianorhabdus maleformis* (Plate VII, 12), *Micula staurophora* (high frequency; Plate VII, 13), and *Watznaueria barnesiae* (Plate VII, 20), but are lacking biostratigraphically significant species, and thus it is difficult to propose a precise age for these deposits based on previously listed calcareous nannoplankton species.

6.1.3. Late Maastrichtian

A single section, namely the upper part of Log 4 (P256–P255 sampling interval), yielded a palynological assemblage that can be assigned to the lower part of upper Maastrichtian. Important dinocyst markers identified in this interval include *Cribroperidinium* sp. A of Brinkhuis and Schiøler (1996) (Plate I, 21), *Deflandrea galeata* (Plate I, 24), *Fibrocysta axialis* (Plate II, 1), *Isabelidinium cooksoniae* (Plate I, 9), *Pierceites? chiemgoviensis* (Plate I, 23), and *Muratodinium fimbriatum* (Plate I, 6). The FOs of *Cribroperidinium* sp. A of Brinkhuis and Schiøler (1996), *Deflandrea galeata* and *Muratodinium fimbriatum*, as well as the LO of *Pierceites? chiemgoviensis* were reported in the lower part of upper Maastrichtian in many areas of the Northern Hemisphere (Schiøler and Wilson, 1993; Schiøler et al., 1997; Slimani, 2000, 2001; Slimani et al., 2010, 2016; Guédé et al., 2014). The dinocyst assemblage in sample P256 also includes taxa such as *Achomosphaera ramulifera* (Plate II, 8), *Areoligera senonensis* (Plate VIII, 2), *Hystrichosphaeridium tubiferum* subsp. *tubiferum* (Plate II, 3), *Leberidocysta chlamydata* (Plate I, 15), *Phelodinium tricuspis* (Plate II, 15), *Trithyrodinium evittii* (Plate IX, 16), all previously encountered in other upper Maastrichtian deposits of the Eastern Carpathians (Țabără and Slimani, 2017; Țabără et al., 2017).

A late Maastrichtian age for sample P255 is also supported by the occurrence of agglutinated foraminifera such as *Caudammina gigantea* (Plate V, 15), *Rzehakina epigona* (Plate VI, 1, 2) and *Gerochammina lenis* (Plate VI, 12). The taxon *Caudammina gigantea* is known to have variable FOs in different basins of the Carpathians (Ion (Săndulescu, 1973; Ion, 1975; Geroch and Nowak, 1984; Neagu, 1990; Kuhnt et al., 1992; Neagu et al., 1992; Cetean et al., 2011), and the high abundances of this species are good indicators for the Upper Cretaceous (Neagu et al., 1992; Olszewska, 1997; Waškowska, 2021). In order to be used in biostratigraphy schemes as an acme, this species must generally account for more than 5% in the assemblage. In sample P255, the percentage recorded by *Caudammina gigantea* is quite small (1.04%), thus limiting the use of this species as an acme in biostratigraphic interpretations. However, based on previous works of Neagu (1990) and Neagu et al. (1992) who proposed the last important biozonation scheme for the Romanian Eastern Carpathians, the occurrence of *Caudammina gigantea* in association with *Rzehakina epigona* and *Gerochammina lenis* allows us to assign the upper part of Log 4 to the upper Maastrichtian.

The calcareous nannoplankton assemblages from the P257–P255 sampling interval (Log 4; Fig. 2) contain three biostratigraphic markers (i.e., *Broinsonia parca parca*, *Ceratolithoides aculeus*, and *Uniplanarius sissinghii*), but only one of them (*Ceratolithoides aculeus*) has a range (66.04–72.05 Ma; Burnett, 1998; Young et al., 2017) that extends into the late Maastrichtian. It is worth mentioning, nevertheless, that typical

late Maastrichtian nannoplankton marker species were not identified within this sampling interval, despite its assessed late Maastrichtian age indicated by the biostratigraphic information provided by palynomorphs and small foraminifera. Furthermore, Campanian and early Maastrichtian marker taxa occurring in the upper part of Log 4 such as *Broinsonia parca parca* and *Uniplanarius sissinghii* should be considered reworked into these younger, upper Maastrichtian deposits.

6.2. Palaeoenvironmental and palaeoecological reconstructions

Palaeoenvironmental and palaeoecological reconstructions of the marine domain where deposits of the Hangu Formation from the upper Upper Campanian–lower upper Maastrichtian stratigraphic interval analyzed in the present study were formed are based primarily on palynofacies constituents, P/G and C/M ratios, as well as the relative abundance of selected dinocyst taxa that are reliable ecological indicators (ranging from nearshore to oceanic, open marine groups of taxa). Furthermore, the terrestrial palynological assemblage recovered from the Hangu Formation deposits also allowed us to outline the palaeoclimatic conditions during this time period. Additional palaeoenvironmental information is provided by the composition of the foraminifera (especially the agglutinated foraminifera) and the calcareous nannoplankton assemblages. A synthetic overview of the resulting assessed palaeoenvironmental/palaeoecological parameters is plotted in Fig. 3.

The kerogen analyzed from the upper Upper Campanian deposits of the Hangu Formation from the study area (sample D260; Log 6) is composed of roughly similar proportions of translucent (~54%) and opaque (~45%) phytoclasts, which are often large in size and lath-shaped, suggesting their relatively short transport and thus nearshore depositional conditions. This interval is characterized by the dominance of peridinioids (65%) over gonyaulacoids, with relatively high values of the P/G ratio (0.65), and a C/M ratio (0.8) reflecting low salinity, nutrient-rich conditions, land proximity, and shallow-water environments. These conclusions are also supported by the predominance of the inner neritic (ING) and nearshore (NG) groups, together reaching up to 86% of the dinocyst assemblage (Fig. 3). The *Isabelidinium* group, including *Isabelidinium cooksoniae* and *Chatangiella? robusta*, dominates, supporting an inner neritic environment relatively close to the coastline for these upper Upper Campanian deposits (Castro and Carvalho, 2015; Chakir et al., 2020).

Palaeoenvironmental conditions quite similar to those described for the Late Campanian persisted up to the Campanian–Maastrichtian transition, as reflected both by the palynological assemblages and the palynofacies composition. A relatively small amount of organic matter of terrestrial origin, represented by equidimensional opaque and translucent phytoclasts, together with a palynological assemblage represented mainly by spores and pollen, has been recognized in the N261–N262 (Log 7) sampling interval. Phytoplankton taxa are almost completely absent in sample N261, but a small number of peridinioid specimens assigned to the *Isabelidinium* group occur in sample N262, reflecting an inner neritic–nearshore environment (Fig. 3). High values of the C/M ratio (e.g., 0.906 in sample N261) also suggests an important continental input and more proximal marine conditions (Carvalho et al., 2016) for the Campanian–Maastrichtian transition in the Pluton–Pipirig area. Nevertheless, redeposition of Campanian–Maastrichtian transition sediments on a more pronounced slope towards deeper-water environments cannot be excluded either, as indicated by the micropalaeontological assemblage recovered from the 63 μm fraction of sample N261. According to our observations, this assemblage is composed of 16 radiolarian individuals referable to the Nassellaria group (Plate VI, 21) alongside poorly diversified agglutinated foraminifera among which the tubular forms represent up to 86%. Abundant siliceous agglutinated tubular taxa (M1 morphogroup) are generally assigned to slope environments (e.g., Jones and Charnock, 1985; Nagy et al., 2000; Murray et al., 2011; Setoyama et al., 2013, 2017) and indicate

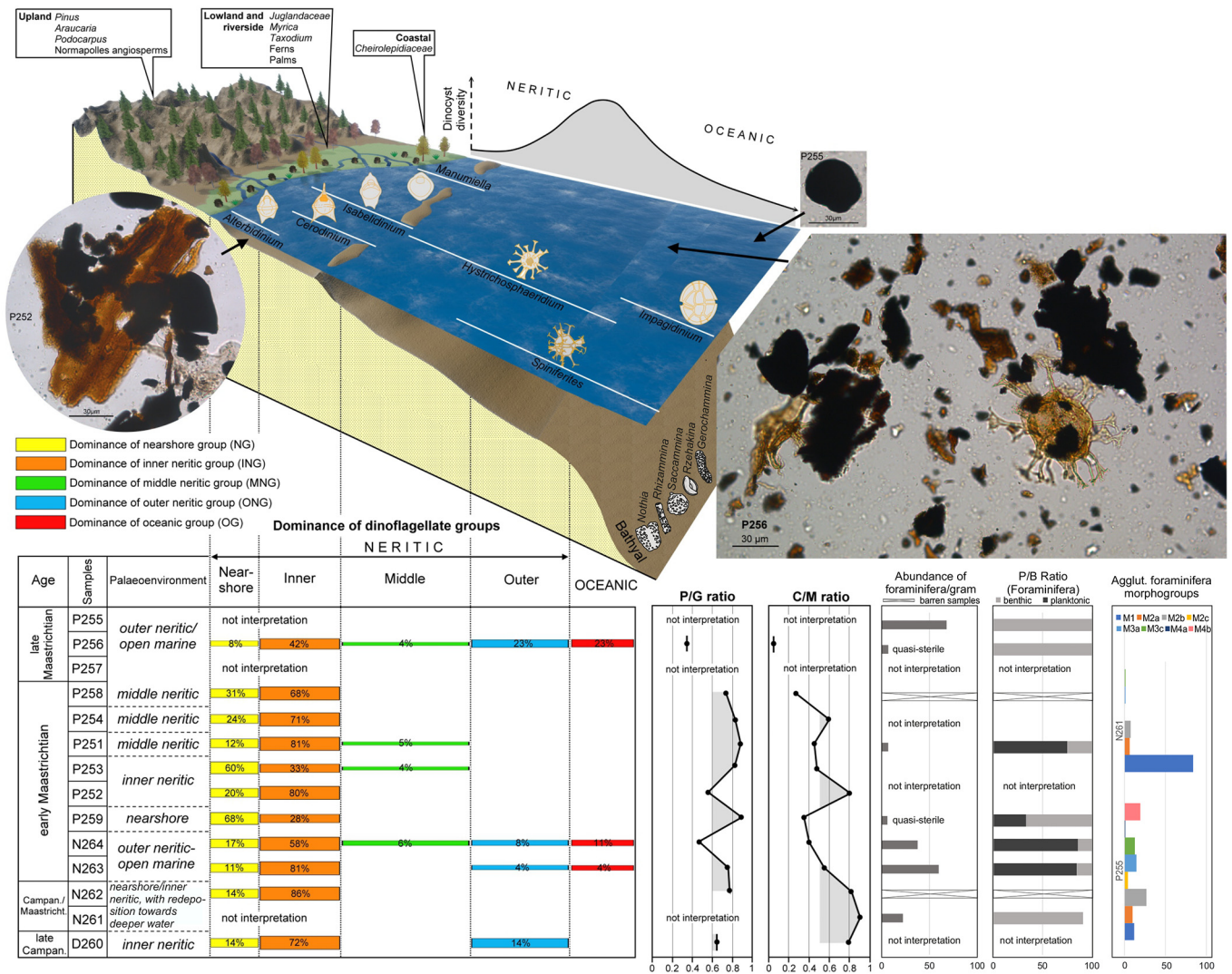


Fig. 3. Model of spatial distribution for the Late Campanian–late Maastrichtian dinocyst ecological groups and selected agglutinated foraminifera through the marine palaeoenvironments of the central-northern Outer Moldavides, as documented by the Hangu Formation in the Pluton-Pipirig area. The vegetation growing in various terrestrial environments, as well as some palynofacies and foraminifera results, are also shown. Abbreviations: P/G – peridinioid/gonyaulacoid dinocysts; C/M – continental/marine palynomorphs; P/B – planktonic/benthonic foraminifera.

palaeoenvironments with bottom waters, low organic matter flux, and moderate oxygenation to the sea floor (Kaminski and Gradstein, 2005; Cetean et al., 2011; Bindu et al., 2013; Setoyama et al., 2017). Together with the presence of radiolarians in the assemblage, such a microfaunal composition could suggest neritic deposition on a steep slope, cold marine waters with a lowered calcium carbonate content (the assemblages are composed only of siliceous forms), and mesotrophic to oligotrophic conditions at the sea floor (low organic matter flux, moderate oxygenation). The lack of calcareous or siliceous microfossils in sample N262 can be attributed to the sedimentation conditions, more precisely to the turbidity currents that actively removed the micropalaeontological assemblages from the sea floor.

Slightly different palaeoenvironmental conditions compared to those recorded around the Campanian–Maastrichtian transition, are documented by the organic matter composition and the palynological assemblages found within the N263–N264 sampling interval (Log 8, northern part of the studied area), which is here assigned to the lower Maastrichtian. Samples from this interval are characterized by a decrease of the P/G ratios (down to 0.45) and the C/M ratios (down to 0.39) (Fig. 3), reflecting more distal conditions within the sedimentary basin. The occurrence of gonyaulacoid dinocysts such as *Pterodinium*

div. sp. and *Spiniferites ramosus*, typical for outer neritic and oceanic groups (Gedl, 2004; Chakir et al., 2020) in sample N264, also support an offshore setting for the deposits of this interval. However, these interpretations are somewhat contrasting with the palynofacies composition observed in sample N263 from the same section, which includes a high proportion of large (frequently larger than 200 μm), lath-shaped and poorly-sorted angular opaque phytoclasts, associated with large particles of woody tissue, features suggesting a short transport of these phytoclasts and thus land proximity during deposition. According to these data, accumulation of the N263–N264 interval deposits took place during the early Maastrichtian within outer neritic–open marine settings with a contribution of redeposited material from the inner neritic zone, consistent with previous observations acknowledging that turbidity currents can occasionally transport organic matter-bearing proximal sediments into distal areas (Tyson, 1995; Oboh-Ikuenobe et al., 1999; McArthur et al., 2016). Additional information related to the palaeobathymetry of these deposits is provided by planktonic foraminifera, as it is well documented that the relative percentage representation of this group usually increases with the distance from the shoreline (van der Zwaan et al., 1990; Murray, 1991, 2006; Spezzaferri et al., 2002; Leckie and Olson, 2003). Even if foraminifera occur in

relatively low numbers in samples N263 and N264, the high abundance percentages recorded by planktonic foraminifera (up to 85%) could be used as an indicator for an outer neritic–bathyal depositional environment.

In the southern part of the study area (Agapei River), the sections represented by logs 1, 2, 3, 5, as well as the lower part of Log 4 also contain deposits assigned to the upper lower Maastrichtian (see the previous chapter, biostratigraphy). Generally, dinocyst assemblages, dominated by peridinioids, are well represented in all samples from these sections, with taxa such as *Alterbidinium* div. sp., *Cerodinium diebelii*, and *Isabelidinium* div. sp. being common. The high abundance of these peridinioid dinocysts, assigned here to the nearshore and inner neritic groups, suggests low salinity (Harris and Tocher, 2003), regressive and shallowing conditions (Tahoun et al., 2018), and/or high levels of nutrients induced by enhanced runoff due to the proximity of the emerged land (Peyrot et al., 2012). In these sections, the gonyaulacoid dinocysts are less abundant. They are mostly represented by *Cladopxydium paucireticulatum*, *Elytrocyta druggii*, *Fromea chytra* and *Spiniferites* sp., associated with rare occurrences of colonial marine algae such as *Palambages morulosa*. The P/G ratio generally shows high values, ranging from 0.89 in sample P259 to 0.74 in sample P258 (Fig. 3), also suggesting nearshore conditions for the interval. The kerogen analyzed from samples P259, P252 and P253 (see Fig. 3 for sample distribution) is composed mainly of occasionally large-sized cutinite and vitrinite mixed with poorly sorted opaque phytoclasts, indicating marginal marine–proximal inner neritic settings, associated with sea-level fall (Steffen and Gorin, 1993). However, close to the lower–upper Maastrichtian transition (samples P251, P254 and P258), equidimensional opaque phytoclasts, small-sized and rounded in shape, become more abundant, frequently exceeding 70% of the total kerogen, thus indicating a slightly longer transport towards the middle neritic areas of the sedimentary basin through the activity of turbidity currents. Sample P259 was quasi-sterile in foraminifera (only a few pyritized tubular foraminifera were identified), while sample P251 yielded a low-abundance assemblage, so that no reliable environmental interpretations were made for these intervals based on this group of microfossils.

A certain dominance of indicators pointing towards the deepening of the depositional area, such as the predominance of gonyaulacoid dinocysts over the peridinioid ones, low values of the P/G and C/M ratios, and a high proportion of opaque phytoclasts assigned to the inertinite group (up to 95% of the total kerogen composition), were recorded in the upper part of Log 4 (P256–P255 sampling interval), dated here as lower upper Maastrichtian. The gonyaulacoid dinocysts are slightly dominant (65% in sample P256), being represented mainly by *Hystriospheridium tubiferum* subsp. *tubiferum*, *Spiniferites ramosus* and *Achomosphaera ramulifera*, all of which reflect more outer neritic/oceanic, open marine environments (Brinkhuis, 1994; Mahboub and Slimani, 2020; Niechwedowicz et al., 2021; Quattrocchio et al., 2021). The highest value of dinocyst species richness was observed also in this interval (30 species in sample P256). The increase in species richness is considered to be indicative of the dinocysts responding to sea level rise (Olde et al., 2015; Maatouf et al., 2020). Such a more distal palaeoenvironment assessed for the late Maastrichtian Hangu sedimentary basin from the study area is also supported by low values of the P/G (0.34) and C/M (0.04) ratios (Fig. 3), as well as by the kerogen composition including mainly opaque phytoclasts that often-present small dimensions and rounded shapes as a result of prolonged transport.

Deep marine environments are also indicated for this section by the foraminifera assemblages that proved to be the best-preserved ones in sample P255. The identified foraminifera individuals have coarse agglutinated tests and large dimensions, and the assemblage presents the highest abundance and diversity. Among them, the representative species of *Aschemocella* (*A. grandis*), *Caudamina* (*C. ovulum*, *C. excelsa*, *C. gigantea*), and *Rzehakina* (*R. epigona*) represent good indicators of bathyal sedimentation areas. *Aschemocella grandis* and *Caudamina*

gigantea were reported from flysch sediments that suggest low terrigenous detrital input in deep-water (predominantly bathyal) and carbonate-poor environments (e.g., Kuhnt et al., 1992; Bâk, 2000; Bâk and Oszczytko, 2000; Kaminski and Gradstein, 2005; Cetean et al., 2011; Bindu et al., 2013; Țabără et al., 2017; Bindu-Haitonic, 2018; Waškowska, 2021), whereas rzehakinids were reported as being restricted to flysch deposits (Kaminski and Gradstein, 2005). The relatively homogeneous distribution of the different foraminifera morphogroups – the highest percentages being reached by the rounded trochospiral and streptospiral and elongate subcylindrical morphotypes – together with the high overall diversity of the foraminifera assemblages suggest relatively good living conditions at the sea floor, with increased organic flux and a moderate level of oxygenation. Thus, the composition of the foraminiferal assemblages (the presence of tubular forms, of the coarsely agglutinated forms, and that of some representative agglutinated species) allows these to be fitted in the “flysch-type” biofacies (Gradstein and Berggren, 1981; Kaminski and Gradstein, 2005), typical for deep marine environments with clastic substrates, where the predominant action is that of turbidity currents. Previous studies of dinoflagellate, foraminifera, and calcareous nannoplankton assemblages, combined with palynofacies analysis, also identified a distal palaeoenvironment during the late Maastrichtian in the northern Moldavidian Domain (Țabără et al., 2017).

In the case of the calcareous nannoplankton assemblages, taking into account that most likely some of the taxa recovered were reworked from older deposits (see above), we chose to briefly characterize the palaeoecological conditions indicated by the main dominant species. Accordingly, the high relative abundance pattern of *Micula staurophora* may suggest a high level of dissolution which affected the composition of the calcareous nannoplankton assemblages, associated with low preservation rates (Hill, 1975; Thierstein, 1976, 1981; Eshet and Almogi-Labin, 1996; Lees, 2002; Foroughi et al., 2016). On the other hand, the relative abundance of *Micula* spp. should be negatively correlated with calcareous nannoplankton species richness and abundance, as a good proxy for original nannoplankton flux in the water column (Thibault and Gardin, 2006). In the largest part of the studied samples *Micula staurophora* indeed shows a negative correlation with species richness, except for two samples, that is, P256 (upper Maastrichtian) in which the abundance of the species was also low, and N262 (Campanian–Maastrichtian transition). Based on these observations one can assume that the original calcareous nannoplankton assemblages were not significantly altered by diagenesis. The taxon *Micula staurophora* is considered by some authors to show preference for cold-water conditions (Doeven, 1983; Watkins and Self-Trail, 2005), although it also may occur in the warm waters of the Tethyan Realm (Koppeh-Dagh Basin, Iran), where it was described to display high abundance values together with *Watznaueria barnesiae* and *Ceratolithoides* spp., in association with a low abundance or even absence of species typically preferring cold waters (*Biscutum magnum*, *Gartnerago segmentatum*, *Kamptnerius magnificus*) (Foroughi et al., 2016). In the northern part of the Eastern Carpathians, deposits of the Hangu Formation present the same abundance pattern for *Micula staurophora* (with a higher relative abundance – up to 87%) as that identified here for the Pluton–Pipirig area, and there this taxon was interpreted as a cold-water indicator (Bindu et al., 2013).

Terrestrial palynomorphs are present mainly in the upper Upper Campanian–lower Maastrichtian deposits of the sections corresponding to logs 1, 2, 3, 5, 6, 7, and 8. The assemblages recovered from these sections are rather similar to other Upper Cretaceous assemblages reported from the Eastern Carpathians (Țabără et al., 2017), the Hațeg Basin (Van Itterbeek et al., 2005; Csiki et al., 2008; Țabără and Slimani, 2019; Botfalvai et al., 2021), and the southwestern Transylvanian Basin (Țabără et al., 2022). In the Pluton–Pipirig area, the upper Upper Campanian–lower Maastrichtian spore/pollen assemblages are characterized by a constant occurrence of *Classopollis*, a pollen type produced by drought-resistant and thermophilous cheirolepidiacean conifers

adapted to arid climatic conditions and to hypersaline soils (Michels et al., 2018). They also contain abundant hygrophytic fern spores (e.g., *Deltoidospora*, *Gleicheniidites*, *Lycopodiumsporites*), together with angiosperm pollen associated with Juglandaceae and other taxa (*Myrica*, palms), indicating plant communities that grew in moist lowland habitats or along river banks. Pollen types characteristic for plants growing in higher altitude areas have rare occurrences in the studied deposits, although a slight increase in the frequency of gymnosperms such as *Araucariacites*, *Pinuspollenites* and *Podocarpidites* was observed at the Campanian–Maastrichtian transition (Log 7, sample N262).

Taxa belonging to the Normapolles group (early angiosperms) occur mainly in the upper Upper Campanian–lower Maastrichtian deposits of the Hangu Formation in the Pluton–Pipirig area, becoming almost absent in the upper Maastrichtian of the studied area. This type of pollen is dominated by species of the genus *Trudopollis* (e.g., *Trudopollis nonperfectus*, *Trudopollis minimus*, *Trudopollis fossulotrudens*), and commonly occurs together with other Normapolles taxa such as *Interporopollenites proporus*, *Oculopollis praedicatus* and *Plicapollis pseudoexcelsus* characterizing “Normapolles Phytogeographic Province”, that extended from southern North America through Europe into western Asia during the Late Cretaceous (Vajda and Bercovici, 2014). In Romania, previous palynological studies have reported assemblages of Normapolles pollen dominated by the genus *Trudopollis*, both in the Upper Campanian–lowermost Maastrichtian deposits of the Hațeg Basin (Țabără and Slimani, 2019; Botfalvai et al., 2021), as well as in the Upper Campanian deposits of the southwestern Transylvanian Basin (Țabără et al., 2022).

Based on the currently available palynological data regarding the distribution of the Late Cretaceous Normapolles group in Romania (Hațeg Basin, Transylvanian Basin, and Eastern Carpathians), we can conclude that the genus *Trudopollis* dominates in this group, with frequent occurrences observed mainly in the Campanian–lower Maastrichtian interval, but becoming almost absent towards the end of the Maastrichtian. Of the Normapolles-producing genera that have been described from Upper Cretaceous deposits of Europe, pollen of the mesofossil genus *Manningia* shares a number of similarities with the Normapolles genus *Trudopollis* (Friis et al., 2011).

7. Conclusions

The study of dinoflagellate cysts, terrestrial palynomorphs, calcareous nannoplankton, foraminifera distributions, and palynofacies in the Upper Cretaceous deposits of the Pluton–Pipirig area (central-northern part of the Eastern Carpathians) belonging to the Hangu Formation led to the following conclusions:

(1) Based on our sampling along eight geological sections (Log 1 to Log 8) covering the Pluton–Pipirig area, these Upper Cretaceous deposits were, for the first time, temporally much better constrained. Based essentially on relevant dinocyst bioevents these deposits are here assigned to the upper Upper Campanian–lower upper Maastrichtian, instead of the Senonian–Paleocene interval as they were loosely dated previously. The presence of upper Upper Campanian deposits is highlighted in the middle part of the Hangu Formation, based on the FOs of *Alterbidinium montanaense*, *Cassiculosphaeridia? intermedia*, and *Diconodinium wilsonii* together with the LO of *Odontochitina operculata*. The upper part of the Hangu Formation is assigned to the lower Maastrichtian–lowermost upper Maastrichtian interval using the FOs of *Alterbidinium varium*, *Isabelidinium cf. bujakii*, and *Cladopyxidium paucireticulatum*, jointly with the LOs of *Alterbidinium acutum*, *Isabelidinium weidichii*, and *Leberidocysta? microverrucosa*. Upper Maastrichtian deposits are recognized within a single section (Log 4) by the FOs of *Cribroperidinium* sp. A of Brinkhuis and Schiøler (1996) and *Deflandrea galeata*, and the LO of *Pierceites? chiemgoviensis*. The late Maastrichtian age at the top of Log 4 is also supported by the occurrence of agglutinated foraminifera taxa such as *Caudamina*

gigantea, *Rzehakina epigona*, and *Gerochammina lenis*. Albeit certain calcareous nannoplankton taxa, such as *Ceratolithoides aculeus* and *Uniplanarius sissinghii*, have sometimes been found useful in biostratigraphic dating, in many cases in the Pluton–Pipirig area such important marker taxa have been shown to be reworked. The synthesis of all of these newly acquired biostratigraphic constraints also allowed the elaboration of a detailed and significantly updated geological map of the study area, previously known for its hydrocarbon accumulations.

(2) The POM analysis of the studied sections revealed an abundance of continental organic matter, with a predominance of translucent phytoclasts (cutinite and vitrinite) over opaque phytoclasts (inertinite) in the otherwise marine upper Upper Campanian–lower Maastrichtian deposits, whereas during the late Maastrichtian, the organic material consists mainly of inertinite. Marine organic matter forms only a minor fraction of the kerogen composition, mainly represented by dinocysts as well as rare occurrences of the granular amorphous organic matter and of foraminifera test linings. Therefore, further geochemical analyses (e.g., gas chromatography–mass spectrometry GC–MS; total organic carbon content) are required for a better understanding of the origin of the organic matter in the middle-upper part of the Hangu Formation, as well as the organic productivity during its deposition.

(3) The POM compositions, the P/G and C/M ratios, and the relative abundance of the different dinocyst eco-groups allow a detailed reconstruction of the palaeoenvironmental history of the central-northern Outer Moldavides in the Pluton–Pipirig sector for the studied time interval. Upper Upper Campanian–lower Maastrichtian sediments were deposited in more proximal marine conditions, as inferred based on palynofacies parameters correlated with the presence of nearshore-inner neritic dinocyst groups. Nevertheless, the transport of organic matter-bearing sediments into the distal area of the basin through turbidity currents was observed within the Log 7 and Log 8 sections, corresponding to the Campanian–Maastrichtian transition and the lower Maastrichtian, respectively. The upper Maastrichtian deposits are typical of outer neritic to distal (bathyal) depositional environments, as indicated by the predominance of small-size opaque phytoclasts with rounded shapes, the higher frequencies of gonyaulacoid dinocysts compared to peridinioids, patterns of dinocyst species richness, low values of P/G and C/M ratios, and high frequency occurrences of deep-water benthic foraminifera. These gradual changes of the palaeoenvironment from more proximal marine conditions that existed during the late Campanian–early Maastrichtian to more distal conditions prevailing during the late Maastrichtian may be related to a transgression and probably a progressive subsidence during this period.

(4) Based on the stratigraphic distribution of the Normapolles group pollen taxa in Romania (Eastern Carpathians, Hațeg Basin, southwestern Transylvanian Basin) during the Late Cretaceous, it appears that certain early angiosperms (e.g., *Manningia*) that are regarded as parent plants of *Trudopollis* spp. proliferated on the emergent landmasses that existed around the present-day Carpathian areas during the Campanian and the early Maastrichtian, but declined towards the end of the Maastrichtian.

Supplementary data to this article can be found online at <https://doi.org/10.1016/j.revpalbo.2023.104878>.

Data availability

The data that has been used is confidential.

Declaration of Competing Interest

The authors declare that they have no known competing financial interests or personal relationships that could have appeared to influence the work reported in this paper.

We the undersigned declare that this manuscript is original, has not been published before and is not currently being considered for publication elsewhere.

We confirm that the manuscript has been read and approved by all named authors and that there are no other persons who satisfied the criteria for authorship but are not listed. We further confirm that the order of authors listed in the manuscript, as well as the corresponding authors, has been approved by all of us.

Daniel Țabără, on behalf of all co-authors.

Acknowledgments

This study was supported by a grant of the Ministry of Research, Innovation and Digitization, CNCS/CCCDI - UEFISCDI, project number PN-III-P4-ID-PCE-2020-2570, within PNCDI III; fieldwork in the Pluton-Pipirig area was also supported by the University of Bucharest grant 10056/2022. The journal Editor-in-Chief José Carrion and the anonymous reviewer are kindly thanked for their comments and suggestions that enhanced the initial manuscript.

References

- Aggarwal, N., 2022. Sedimentary organic matter as a proficient tool for the palaeoenvironmental and palaeodepositional settings on Gondwana coal deposits. *J. Petrol. Explor. Prod. Technol.* 12, 257–278. <https://doi.org/10.1007/s13202-021-01331-x>.
- Antonescu, E., Alexandrescu, G., 1979. Données préliminaires sur les dinoflagellés des couches de Hangu (Sénonien-Paléocène). *Dări de Seamă ale Institutului de Geologie și Geofizică* 66, 61–93.
- Antonescu, E., Foucher, J.-C., Odin, G.S., 2001a. Les kystes de dinoflagellés de la carrière de Tercis les Bains (Landes, France). In: Odin, G.S. (Ed.), *The Campanian-Maastrichtian Stage Boundary: Characterisation at Tercis les Bains (France) and Correlation with Europe and Other Continents. Developments in Palaeontology and Stratigraphy* vol. 19. Elsevier, Amsterdam, pp. 235–252.
- Antonescu, E., Foucher, J.-C., Odin, G.S., Schiøler, P., Siegl-Farkas, A., Wilson, G.J., 2001b. Dinoflagellate cysts in the Campanian-Maastrichtian succession of Tercis les Bains (Landes, France), a synthesis. In: Odin, G.S. (Ed.), *The Campanian-Maastrichtian Stage Boundary: Characterisation at Tercis les Bains (France) and Correlation with Europe and Other Continents. Developments in Palaeontology and Stratigraphy* vol. 19. Elsevier, Amsterdam, pp. 253–264.
- Aurisano, R.W., 1989. Upper Cretaceous dinoflagellate biostratigraphy of the subsurface Atlantic Coastal Plain of New Jersey and Delaware, U.S.A. *Palynology* 13, 143–179. <https://doi.org/10.1080/01916122.1989.9989359>.
- Bădescu, D., 2005. Evoluția tectono-stratigrafică a Carpaților Orientali în decursul Mezozoicului și Neozoicului. Editura Economică, București, p. 312.
- Bağ, K., 2000. Biostratigraphy of deep-water agglutinated foraminifera in Scaglia Rossa-type deposits, the Pieniny Klippen Belt, Carpathians, Poland. In: Hart, M., Kaminski, M.A., Smart, C. (Eds.), *Proceedings of the Fifth International Workshop on Agglutinated Foraminifera*. Grzybowski Foundation Spec. Publ. 7, pp. 15–41.
- Bağ, K., Oszczytko, N., 2000. Late Albian and Cenomanian redeposited foraminifera from Late Cretaceous-Palaeocene deposits of the Raca Subunit (Magura Nappe, Polish Western Carpathians) and their paleogeographical significance. *Geol. Carpath.* 51 (6), 371–382.
- Baraboshkin, E.Y., Guzhikov, A.Y., Aleksandrova, G.N., Fomin, V.A., Pokrovsky, B.G., Grishchenko, V.A., Manikin, A.G., Naumov, E.V., E.V., 2020. New sedimentological, magnetostratigraphic, and biostratigraphic data on the Campanian-Maastrichtian of Beshkosh Mountain, southwest Crimea. *Stratigr. Geol. Correl.* 28 (8), 816–858. <https://doi.org/10.1134/S0869593820060040>.
- Batten, D.J., 1999. Small palynomorphs. In: Jones, T.P., Rowe, N.P. (Eds.), *Fossil Plants and Spores: Modern Techniques*. Geological Society, London, pp. 15–19.
- Bijl, P.K., Guerin, G.R., Sanmiguel Jaimes, E.A., Sluijs, A., Casadio, S., Valencia, V., Amenábar, C.R., Encinas, A., 2021. Campanian–Eocene dinoflagellate cyst biostratigraphy in the Southern Andean foreland basin: implications for Drake Passage throughflow. *Andean Geol.* 48 (2), 185–218. <https://doi.org/10.5027/andgeoV48n2-3339>.
- Bindiu, R., Filipescu, S., Bălc, R., 2013. Biostratigraphy and paleoenvironment of the Upper Cretaceous deposits in the northern Tarcău Nappe (Eastern Carpathians) based on foraminifera and calcareous nanoplankton. *Geol. Carpath.* 64 (2), 117–132. <https://doi.org/10.2478/geoca-2013-0008>.
- Bindiu, R., Filipescu, S., Bălc, R., Cocis, L., Gligor, D., 2016. The middle/late Eocene transition in the Eastern Carpathians (Romania) based on foraminifera and calcareous nanofossil assemblages. *Geol. Quart.* 60 (1), 38–55. <https://doi.org/10.7306/gq.1237>.
- Bindiu-Haitonic, R., 2018. Relația dintre asociațiile de foraminifere fosile și mediile depozitionale din Nordul Pânzei de Tarcău (Carpații Orientali, România). *Presa Universitară Clujeană*, p. 237.
- Bindiu-Haitonic, R., Niculici, S., Filipescu, S., Bălc, R., Aroldi, C., 2017. Biostratigraphy and paleoenvironments of the Eocene deep-water deposits of the Tarcău Nappe (Eastern Carpathians, Romania) based on agglutinated foraminifera and calcareous nanofossil assemblages. In: Kaminski, M.A., Alegret, L. (Eds.), *Proceedings of the Ninth International Workshop on Agglutinated Foraminifera*. Grzybowski Foundation Special Publication, 22, pp. 15–35.
- Bindiu-Haitonic, R., Filipescu, S., Aroldi, C., Oltean, G., Chira, C.M., 2019. Eocene Deep Water foraminifera from the Eastern Carpathians (Romania). *Paleoenvironments and biostratigraphical remarks*. *Micropaleontology* 65 (1), 47–61. <https://doi.org/10.47894/mpal.65.1.03>.
- Bojar, A.V., Bojar, H.P., 2013. The Cretaceous–Paleogene boundary in the East Carpathians, Romania: evidence from geochemistry, mineralogy and calcareous nanofossils. In: Bojar, A.V., Melinte-Dobrinescu, M.C., Smit, J. (Eds.), *Isotopic Studies in Cretaceous Research*. Geological Society, London, Special Publications 382, pp. 105–122. <https://doi.org/10.1144/SP382.11>.
- Bojar, A.V., Melinte-Dobrinescu, M.C., Bojar, H.P., 2009. A continuous Cretaceous–Paleogene red bed section in the Romanian Carpathians. In: Hu, X., Wang, C., Scott, R.W., Wagreich, M., Jansa, L. (Eds.), *Cretaceous Oceanic Red Beds: Stratigraphy, Composition, Origins, and Paleogeographic and Paleoclimatic Significance*. SEPM, Special Publications 91, pp. 121–135.
- Botfalvai, G., Csiki-Sava, Z., Kocsis, L., Albert, G., Magyar, J., Bodor, E.R., Țabără, D., Ulyanov, A., Makádi, L., 2021. ‘X’ marks the spot! Sedimentological, geochemical and palaeontological investigations of Upper Cretaceous (Maastrichtian) vertebrate fossil localities from the Vălioara valley (Densus–Ciula Formation, Hațeg Basin, Romania). *Cretac. Res.* 123, 104781. <https://doi.org/10.1016/j.cretres.2021.104781>.
- Bown, P.R., Young, J.R., 1998. Introduction. In: Bown, P.R. (Ed.), *Calcareous Nanofossil Biostratigraphy*. British Micropaleont. Soc. Ser. Chapman & Hall, London, pp. 1–15.
- Bratu, E., 1965. Microbiostratigrafia Cretacicului Superior din zona Șisturilor Negre cuprinsă între Covasna și Valea Buzăului. *Dări de Seamă ale Institutului de Geologie și Geofizică* 52 (2), 209–228.
- Brinkhuis, H., 1994. Late Eocene to Early Oligocene dinoflagellate cysts from the Priabonian type-area (northeast Italy): biostratigraphy and paleoenvironmental interpretation. *Palaeogeogr. Palaeoclimatol. Palaeoecol.* 107 (1), 121–163. [https://doi.org/10.1016/0031-0182\(94\)90168-6](https://doi.org/10.1016/0031-0182(94)90168-6).
- Brinkhuis, H., Bujak, J.P., Smit, J., Versteegh, G.J.M., Visscher, H., 1998. Dinoflagellate-based sea surface temperature reconstructions across the Cretaceous–Tertiary boundary. *Palaeogeogr. Palaeoclimatol. Palaeoecol.* 141, 67–83. [https://doi.org/10.1016/S0031-0182\(98\)00004-2](https://doi.org/10.1016/S0031-0182(98)00004-2).
- Burnett, J.A., 1999. Upper Cretaceous. In: Bown, P.R. (Ed.), *Calcareous Nanofossils Biostratigraphy*. British Micropaleontology Society Series. Chapman and Hall, London, pp. 132–199.
- Carvalho, M.A., Cabral Ramos, R.R., Crud, M.B., Witovisk, L., Kellner, A.W.A., Silva, H.P., Grillo, O.N., Riff, D., Romano, P.S.R., 2013. Palynofacies as indicators of paleoenvironmental changes in a Cretaceous succession from the Larsen Basin, James Ross Island, Antarctica. *Sediment. Geol.* 295, 53–66. <https://doi.org/10.1016/j.sedgeo.2013.08.002>.
- Carvalho, M.A., Bengtson, P., Lana, C.C., 2016. Late Aptian (Cretaceous) paleoceanography of the South Atlantic Ocean inferred from dinocyst communities of the Sergipe Basin, Brazil. *Paleoceanography* 31, 2–26. <https://doi.org/10.1002/2014PA002772>.
- Castro, S.P., Carvalho, M.A., 2015. Santonian dinocyst assemblages of the Santa Marta Formation, Antarctic Peninsula: inferences for paleoenvironments and paleoecology. *Anais da Academia Brasileira de Ciências* 87 (3), 1583–1597. <https://doi.org/10.1590/0001-3765201520140651>.
- Cetean, C., Bălc, R., Kaminski, M.A., Filipescu, S., 2011. Integrated biostratigraphy and paleoenvironments of an upper Santonian–upper Campanian succession from the southern part of the Eastern Carpathians, Romania. *Cretac. Res.* 32, 575–590. <https://doi.org/10.1016/j.cretres.2010.11.001>.
- Chakir, S., Slimani, H., Hssaida, T., Kocsis, L., Gheerbrant, E., Bardet, N., Jalil, N.-E., Moufih, M., Mahboub, I., Jbari, H., 2020. Dinoflagellate cyst evidence for the age, paleoenvironment and paleoclimate of a new Cretaceous–Paleogene (K/Pg) boundary section at the Bou Angueur syncline, Middle Atlas, Morocco. *Cretaceous Res.* 106, 104221. <https://doi.org/10.1016/j.cretres.2019.104219>.
- Constantinescu, E., Anastasiu, N., 2019. *Resursele minerale ale României, Resurse energetice* (vol. III). Editura Academiei Române, p. 648.
- Csiki, Z., Ionescu, A., Grigorescu, D., 2008. The Budurone microvertebrate site from the Maastrichtian of the Hațeg Basin – flora, fauna, taphonomy and paleoenvironment. *Acta Palaeontol. Roman.* 6, 49–66.
- Doeven, P.H., 1983. Cretaceous nanofossil stratigraphy and paleoecology of the Canadian Atlantic Margin. *Bull. Geol. Surv. Can.* 356, 1–70.
- Ercegovac, M., Kostić, A., 2006. Organic facies and palynofacies: nomenclature, classification and applicability for petroleum source rock evaluation. *Int. J. Coal Geol.* 68, 70–78. <https://doi.org/10.1016/j.coal.2005.11.009>.
- Eshet, Y., Almogi-Labin, A., 1996. Calcareous nanofossils as paleoproductivity indicators in Upper Cretaceous organic-rich sequences in Israel. *Mar. Micropaleontol.* 29 (1), 37–61. [https://doi.org/10.1016/0377-8398\(96\)00006-0](https://doi.org/10.1016/0377-8398(96)00006-0).
- Eshet, Y., Almogi-Labin, A., Bein, A., 1994. Dinoflagellate cysts, paleoproductivity and upwelling systems: a Late Cretaceous example from Israel. *Mar. Micropaleontol.* 23 (3), 231–240. [https://doi.org/10.1016/0377-8398\(94\)90014-0](https://doi.org/10.1016/0377-8398(94)90014-0).
- Firth, J.V., 1987. Dinoflagellate biostratigraphy of the Maastrichtian to Danian interval in the U.S. Geological Survey Albany core, Georgia, U.S.A. *Palynology* 11, 199–216. <https://doi.org/10.1080/01916122.1987.9989328>.
- Fisher, R.A., Corbet, A.S., Williams, C.B., 1943. The relationship between the number of species and the number of individuals in a random sample of an animal population. *J. Anim. Ecol.* 12, 42–58.
- Foroughi, F., Gardin, S., Kani, A.L., 2016. Campanian calcareous nanofossil biostratigraphy of eastern Koppeh-Dagh basin (North East of Iran), Tethyan realm. *Riv. Ital. Paleontol. Stratigr.* 122 (3), 165–184. <https://doi.org/10.13130/2039-4942/7739>.
- Friis, E.M., Crane, P.R., Pedersen, K.R., 2011. *Early Flowers and Angiosperm Evolution*. Cambridge University Press, p. 585.
- Gedl, P., 2004. Dinoflagellate cyst record of the deep-sea Cretaceous–Tertiary boundary at Uzgrun, Carpathian Mountains, Czech Republic. *Geol. Soc. Spec. Publ.* 230, 257–273.
- Geroch, S., Nowak, W., 1984. Proposal of zonation for the late Tithonian–late Eocene, based upon arenaceous foraminifera from the outer Carpathians, Poland. In: Oertli, H.J. (Ed.), *Benthos '83, 2nd International Symposium on Benthic Foraminifera* (Pau 1983). Elf Aquitaine, Esso REP, and Total CFP, Pau and Bordeaux, pp. 225–239.

- Góczán, F., Siegl-Farkas, A., 1990. Palynostratigraphical zonation of the Senonian sediments in Hungary. *Rev. Palaeobot. Palynol.* 66, 361–377. [https://doi.org/10.1016/0034-6667\(90\)90047-M](https://doi.org/10.1016/0034-6667(90)90047-M).
- Gradstein, F.M., Berggren, W.A., 1981. Flysch-type agglutinated foraminifera and the Maastrichtian to Paleogene history of the Labrador and North Seas. *Mar. Micropaleontol.* 6, 211–268.
- Grasu, C., Catană, C., Grinea, D., 1988. *Flîșul carpatic. Petrografie și considerații economice*. Editura Tehnică, București, p. 208.
- Guédé, K.E., Slimani, H., Louwyse, S., Asebriy, L., Toufiqu, A., Ahmamou, M., Amrani, El, El Hassani, I.E., Digbehi, Z.B., 2014. Organic-walled dinoflagellate cysts from the Upper Cretaceous–lower Paleocene succession in the western External Rif, Morocco: new species and new biostratigraphic results. *Geobios* 47, 291–304. <https://doi.org/10.1016/j.geobios.2014.06.006>.
- Hammer, Ø., Harper, D.A.T., 2006. *Paleontological Data Analysis*. Blackwell Publishing, Oxford, p. 351.
- Harris, A.J., Tocher, B.A., 2003. Palaeoenvironmental analysis of late Cretaceous dinoflagellate cyst assemblages using high-resolution sample correlation from the Western Interior Basin, USA. *Mar. Micropaleontol.* 48, 127–148.
- Hill, M.E., 1975. Selective dissolution of mid-Cretaceous (Cenomanian) calcareous nanofossils. *Micropaleontology* 21 (2), 227–235.
- Ion, J., 1975. Microbiostratigraphie, associations et zones a foraminifères du Crétacé du flysch externe des Carpates Orientales (Roumanie). *Rev. Esp. Micropaleontol.* 7 (1), 99–111.
- Ion (Săndulescu), J., 1973. Étude micropaléontologique et stratigraphique du flysch du Crétacé supérieur-Paléocène de la région de Brețcu-Comandău (Secteur intern meridional de la nappe de Tarcău-Carpates Orientales). Institutul Geologic, Memorii 17, pp. 1–52 Bucharest.
- Ion, J., Antonescu, E., Micu, M., 1982. On the Paleocene of the Bistrița Half-window (East Carpathians). *Dări de seamă ale ședințelor, Institutul Geologic și Geofizică* 69 (4), 117–136.
- Ionesi, L., 1966. Contributions to the Cretaceous–Paleogene boundary from external flysch zone of the Eastern Carpathians. *Analele Științifice ale Universității “Al. I. Cuza” Iași, sect. IIb, Geologie-Geografie* 12, 81–90 (in Romanian).
- Ionesi, L., 1975. Limite Maestrichtien-Paléocène et Cuisien nummulitique dans le flysch de Bucovine. 14-th European Micropaleontological Colloquium, *Micropaleontological Guide to the Mesozoic and Tertiary of the Romanian Carpathians*. Published by the Institute of Geology and Geophysics, Bucharest, pp. 145–150.
- Ionesi, L., Todorjescu, M., 1968. Microfaunistic data on the Cretaceous–Paleogene boundary in the outer flysch from Moldova Valley basin. *Analele Științifice ale Universității “Al. I. Cuza” Iași, sect. II, Geologie-Geografie* 14, 61–68 (in Romanian).
- Jbari, H., Slimani, H., Chekar, M., Asebriy, L., Benzaggagh, M., Mahboub, I., Chakir, S., 2020. Campanian to Danian dinoflagellate cyst assemblages from the southwestern Tethyan margin (Tattofte section, western External Rif, Morocco): biostratigraphic and paleobiogeographic interpretations. *Rev. Palaeobot. Palynol.* 279, 104225. <https://doi.org/10.1016/j.revpalbo.2020.104225>.
- Joja, T., Chiriac, M., 1964. Asupra prezenței unor amoniți în Stratele de Hangu din flîșul extern de la Putna. *Studii și Cercetări de Geologie, Geofizică, Geografie* 9 (1), 39–49.
- Jones, R.W., Charnock, M.A., 1985. “Morphogroups” of agglutinating foraminifera. Their life position and feeding habits and potential applicability in (paleo)ecological studies. *Rev. Paleobiol.* 4 (2), 311–320.
- Juravle, D.T., Ursu, A., Chelariu, C., Juravle, V., 2019. Distribution of Cretacic / Miocene petrofacies at the contact of the Carpathian Orogen and Moldavian Platform. Morphometric particularities of the mountain-plateau relief transition, between Suceava and Moldova Valley (Obcina Mare/Suceava Plateau, Romania). 19th International Multidisciplinary Scientific GeoConference SGEM 2019, Conference Proceedings v. 19, issue 1.1, Bulgaria, pp. 147–161. <https://doi.org/10.5593/sgem2019/1.1/S01.019>.
- Kaminski, M.A., Gradstein, F.M., 2005. Atlas of Paleogene cosmopolitan deep-water agglutinated foraminifera. *Grzybowski Foundation* 10, 574 + vii pp.
- Kirsch, K.-H., 1991. Dinoflagellatenzyklen aus der Oberkreide des Helvetikums und Nordultrahelvetikums von Oberbayern. *Münchner Geowissenschaftliche Abhandlungen, Reihe A: Geologie und Paläontologie* 22, 1–306.
- Kuhnt, W., Geroch, S., Kaminski, M.A., Moullade, M., Neagu, T., 1992. Upper Cretaceous Abyssal claystones in the North Atlantic and the western Tethys - current status of biostratigraphical correlation using agglutinated foraminifers. *Cretac. Res.* 13, 467–478. [https://doi.org/10.1016/0195-6671\(92\)90011-E](https://doi.org/10.1016/0195-6671(92)90011-E).
- Leckie, R.M., Olson, H.C., 2003. Foraminifera as proxies for sea-level change on siliclastic margins. In: Olson, H.C., Leckie, R.M. (Eds.), *Micropaleontologic Proxies for Sea-Level Change and Stratigraphic Discontinuities*. SEPM Society for Sedimentary Geology, SEPM Special Publication 75, pp. 5–19. <https://doi.org/10.2110/pec.03.75.0005>.
- Lees, J.A., 2002. Calcareous nanofossil biogeography illustrates palaeoclimate change in the Late Cretaceous Indian Ocean. *Cretac. Res.* 23, 537–634. <https://doi.org/10.1006/cres.2003.1021>.
- Leever, K.A., Mațenco, L., Bertotti, G., Cloetingh, S., Drijkoningen, G.G., 2006. Late orogenic vertical movements in the Carpathian Bend Zone - seismic constraints on the transition zone from orogen to foredeep. *Basin Res.* 18, 521–545. <https://doi.org/10.1111/j.1365-2117.2006.00306.x>.
- Maatouf, W., Hssaïda, T., Benbouziane, A., Khaffou, H., Essamoud, R., 2020. Late Aptian to early Cenomanian dinoflagellate cysts from Agadir Basin, southwestern Morocco: biostratigraphy and palaeoenvironment. *Ann. Paléontol.* 106 (4), 102441. <https://doi.org/10.1016/j.annpal.2020.102441>.
- Machaniec, E., Kowalczywska, O., Jugowicz, M., Gasiński, M.A., Uchman, A., 2020. Foraminiferal and calcareous nannoplankton bioevents and changes at the Late Cretaceous–earliest Paleogene transition in the northern margin of Tethys (Hyzne section, Polish Carpathians). *Geol. Quart.* 64 (3), 567–588.
- Macovei, G., Atanasiu, I., 1925. Structure géologique de la vallée de la Bistrița. *C.R. Inst. Géol. Roum.* VIII, București.
- Mahanipour, A., Mutterlose, J., Parandavar, M., 2022. Integrated bio- and chemostratigraphy of the Cretaceous–Paleogene boundary interval in the Zagros Basin (Iran, Central Tethys). *Palaeogeogr. Palaeoclimatol. Palaeoecol.* 587, 110785. <https://doi.org/10.1016/j.palaeo.2021.110785>.
- Mahboub, I., Slimani, H., 2020. Middle Eocene dinoflagellate cysts from the Tsoul section, eastern External Rif, Morocco: biostratigraphy and paleoenvironmental interpretations. *Arab. J. Geosci.* 13, 197. <https://doi.org/10.1007/s12517-020-5165-7>.
- Malata, E., 2002. Albian–Early Miocene foraminiferal assemblages of the Magura Nappe (Polish Outer Carpathians). *Geol. Carpath.* 53, 77–79.
- Marheinecke, U., 1986. *Dinoflagellaten des Maastrichtium der Grube Hemmoor (Niedersachsen)*. *Geol. Jah. A* 93, 3–93.
- May, F.E., 1980. Dinoflagellate cysts of the Gymnodiniaceae, Peridiniaceae, and Gonyaulacaceae from the Upper Cretaceous Monmouth Group, Atlantic Highlands, New Jersey. *Palaeontogr. Abt. B* 172 (1–4), 10–116.
- McArthur, A.D., Kneller, B.C., Wakefield, M.I., Souza, P.A., Kuchle, J., 2016. Palynofacies classification of the depositional elements of confined turbidite systems: examples from the Gres d’Annot, SE France. *Mar. Pet. Geol.* 77, 1254–1273. <https://doi.org/10.1016/j.marpetgeo.2016.08.020>.
- Melinte, M.C., Jipa, D., 2005. Campanian–Maastrichtian marine red beds in Romania: biostratigraphic and genetic significance. *Cretac. Res.* 26, 49–56. <https://doi.org/10.1016/j.cretres.2004.11.002>.
- Melinte-Dobrinescu, M.C., Roban, R.D., Stoica, M., 2015. Palaeoenvironmental changes across the Albian–Cenomanian boundary interval of the Eastern Carpathians. *Cretac. Res.* 54, 68–85. <https://doi.org/10.1016/j.cretres.2014.10.010>.
- Mendonça Filho, J.G., Menezes, T.R., Mendonça, J.O., 2011. Organic composition (Palynofacies Analysis) (Chapter 5). ICCP Training Course on Dispersed Organic Matter, pp. 33–81.
- Michels, F.H., Alves de Souza, P., Premaor, E., 2018. Aptian–Albian palynologic assemblages interbedded within salt deposits in the Espírito Santo Basin, eastern Brazil: biostratigraphical and paleoenvironmental analysis. *Mar. Pet. Geol.* 91, 785–799. <https://doi.org/10.1016/j.marpetgeo.2018.01.023>.
- Mohamed, O., Wagreich, M., 2013. Organic-walled dinoflagellate cyst biostratigraphy of the Well Höfllein 6 in the Cretaceous–Paleogene Rhenodanubian Flysch Zone (Vienna Basin, Austria). *Geol. Carpath.* 64 (3), 209–230. <https://doi.org/10.2478/geoca-2013-0015>.
- Morgiel, J., Olszewska, B., 1981. Biostratigraphy of the Polish External Carpathians based on agglutinated foraminifera. *Micropaleontology* 27, 1–30.
- Murgeanu, G., Mirăuță, O., 1968. *Piatra Neamț sheet (geological map, scale 1:200000)*. Institutul Geologic al României.
- Murray, J.W., 1991. *Ecology and Paleoecology of Benthic Foraminifera*. Longman Scientific and Technical, Avon, p. 397.
- Murray, J.W., 2006. *Ecology and Applications of Benthic Foraminifera*. Cambridge University Press, p. 462.
- Murray, J.W., Alve, E., Jones, B.W., 2011. A new look at modern agglutinated benthic foraminiferal morphogroups: their value in palaeoecological interpretation. *Palaeogeogr. Palaeoclimatol. Palaeoecol.* 309 (3–4), 229–241. <https://doi.org/10.1016/j.palaeo.2011.06.006>.
- Nagy, J., Kaminski, M.A., Kuhnt, W., Bremer, M.A., 2000. Agglutinated foraminifera from neritic to bathyal facies in the Palaeogene of Spitsbergen and the Barents Sea. In: Hart, M.B., Kaminski, M.A. (Eds.), *Proceedings of the Fifth International Workshop on Agglutinated Foraminifera*. Grzybowski Foundation Special Publication, 7, pp. 333–361.
- Neagu, T., 1990. *Gerochammina* n.gen. and related genera from the Upper Cretaceous flysch-type benthic foraminiferal fauna, Eastern Carpathians – Romania. In: Hemleben, C., Kaminski, M.A., Kuhnt, W., Scott, D.B. (Eds.), *Paleoecology, Biostratigraphy, Paleoceanography and Taxonomy of Agglutinated Foraminifera*. 327. NATO ASI C, pp. 245–265.
- Neagu, T., Platon, E., Dumitrescu, G., Selea, A., 1992. The biostratigraphical significance of agglutinated foraminifera in the Eastern Carpathians (Upper Cretaceous). *Analele Universității București* 15–16, 45–49.
- Niechwedowicz, M., 2019. *Odontochitina dilatata* sp. nov. from the Campanian (Upper Cretaceous) of Poland: the importance of wall structure in the taxonomy of selected ceratitacean dinoflagellate cysts. *Palynology* 43 (3), 423–450. <https://doi.org/10.1080/01916122.2018.1458754>.
- Niechwedowicz, M., Walaszczyk, I., 2022. Dinoflagellate cysts of the upper Campanian–basal Maastrichtian (Upper Cretaceous) of the Middle Vistula River section (central Poland): stratigraphic succession, correlation potential and taxonomy. *Newsl. Stratigr.* 55 (1), 21–67. <https://doi.org/10.1127/nos/2021/0639>.
- Niechwedowicz, M., Walaszczyk, I., Barski, M., 2021. Phytoplankton response to palaeoenvironmental changes across the Campanian–Maastrichtian (Upper Cretaceous) boundary interval of the Middle Vistula River section, central Poland. *Palaeogeogr. Palaeoclimatol. Palaeoecol.* 577, 110558. <https://doi.org/10.1016/j.palaeo.2021.110558>.
- Oboh-Ikenobe, F.E., Hoffmeister, A.P., Chrisfield, R.A., 1999. Cyclical distribution of dispersed organic matter and dinocysts, ODP site 959 (early Oligocene–early Miocene, Côte d’Ivoire–Ghana transform margin). *Palynology* 23, 87–96.
- Ogg, J.G., Hinnov, L.A., Huang, C., 2012. Cretaceous. In: Gradstein, F.M., Ogg, J.G., Schmitz, M.D., Ogg, G.M. (Eds.), *The Geologic Time Scale 2012*. Elsevier, pp. 793–853. <https://doi.org/10.1016/B978-0-444-59425-9.00027-5>.
- Olaru, L., 1978. Research on the stratigraphic distribution of microflora in the Paleogene flysch between Bistrița and Troțuș Valleys. *Institut de Géologie et de Géophysique, Mémoires* 27, 5–111 (In Romanian).
- Olde, K., Jarvis, I., Uličný, D., Pearce, M.A., Trabucho-Alexandre, J., Čech, S., Gröcke, D.R., Laurin, J., Švábenická, L., Tocher, B.A., 2015. Geochemical and palynological sea-level proxies in hemipelagic sediments: A critical assessment from the Upper Cretaceous of the Czech Republic. *Palaeogeogr. Palaeoclimatol. Palaeoecol.* 435, 222–243.

- Olszewska, B., 1997. Foraminiferal biostratigraphy of the Polish Outer Carpathians: a record of basin geohistory. *Ann. Soc. Geol. Pol.* 67, 325–337.
- Oszczypko, N., Malata, E., Bał, K., Kędzierski, M., Oszczypko-Clowes, M., 2005. Lithostratigraphy and biostratigraphy of the Upper Albian-Lower/Middle Eocene flysch deposits in the Bystrica and Rača subunits of the Magura Nappe (Beskid Wyspowy and Gorce Ranges; Poland). *Ann. Soc. Geol. Pol.* 75, 27–69.
- Pellaton, C., Gorin, G.E., 2005. The Miocene New Jersey passive margin as a model for the distribution of sedimentary organic matter in siliciclastic deposits. *J. Sediment. Res.* 75, 1011–1027.
- Peyrot, D., Barroso-Barcenilla, F., Feist-Burkhardt, S., 2012. Palaeoenvironmental controls on late Cenomanian–early Turonian dinoflagellate cyst assemblages from Condemios (Central Spain). *Rev. Palaeobot. Palynol.* 180, 25–40. <https://doi.org/10.1016/j.revpalbo.2012.04.008>.
- Peyrot, D., Barrón, E., Pereda-Suberbiola, X., Company, J., 2020. Vegetational composition of the Upper Cretaceous vertebrate site of Chera (Valencia, Spain) and its significance in mosaic vegetation from southwestern Europe. *Cretac. Res.* 106, 104254. <https://doi.org/10.1016/j.cretres.2019.104254>.
- Polette, F., Batten, D.J., 2017. Fundamental reassessment of the taxonomy of five Normapolles pollen genera. *Rev. Palaeobot. Palynol.* 243, 47–91. <https://doi.org/10.1016/j.revpalbo.2017.04.001>.
- Pross, J., Brinkhuis, H., 2005. Organic-walled dinoflagellate cysts as paleoenvironmental indicators in the Paleogene; a synopsis of concepts. *Paläontol. Z.* 79 (1), 53–59.
- Quattrocchio, M.E., Martínez, M.A., Umazano, A.M., Tamame, M.A., Agüero, L., 2021. The Danian Sea: Dinoflagellate cysts assemblages from Neuquén Basin, Roca Formation (Argentina) and its comparison with other southern South America localities. *J. S. Am. Earth Sci.* 111, 103469. <https://doi.org/10.1016/j.jsames.2021.103469>.
- Răbăgia, T., Roban, R.D., Tărăpoancă, M., 2011. Sedimentary records of Paleogene (Eocene to Lowermost Miocene) deformations near the contact between the Carpathian thrust belt and Moesia. *Oil Gas Sci. Technol.* 66, 931–952.
- Radmacher, W., Pérez-Rodríguez, I., Arz, J.A., Pearce, M.A., 2014. Dinoflagellate biostratigraphy at the Campanian–Maastrichtian boundary in Zumaia, northern Spain. *Cretac. Res.* 51, 309–320. <https://doi.org/10.1016/j.cretres.2014.07.004>.
- Radmacher, W., Kobos, K., Tyszką, J., Jarzyńska, A., Arz, J.A., 2020. Palynological indicators of palaeoenvironmental perturbations in the Basque–Cantabrian Basin during the latest Cretaceous (Zumaia, northern Spain). *Mar. Pet. Geol.* 112, 104107. <https://doi.org/10.1016/j.marpetgeo.2019.104107>.
- Roban, R.D., Krézsek, C., Melinte-Dobrinescu, M.C., 2017. Cretaceous sedimentation in the outer Eastern Carpathians: implications for the facies model reconstruction of the Moldavide Basin. *Sediment. Geol.* 354, 24–42. <https://doi.org/10.1016/j.sedgelo.2017.04.001>.
- Săndulescu, M., 1984. *Geotectonica României*. Editura Tehnică, București, p. 336.
- Săndulescu, M., Ștefănescu, M., Butac, A., Pătruț, I., Zaharescu, P., 1981. Genetical and structural relations between Flysch and Molasse. *Guidebook Series of the Geological Institute of Romania*. 19, pp. 3–94.
- Schiøler, P., Wilson, G.J., 1993. Maastrichtian dinoflagellate zonation in the Dan Field, Danish North Sea. *Rev. Palaeobot. Palynol.* 78, 321–351.
- Schiøler, P., Wilson, G.J., 2001. Dinoflagellate biostratigraphy around the Campanian–Maastrichtian boundary at Tercis Les Bains, southwest France. In: Odin, G.S. (Ed.), *The Campanian–Maastrichtian Stage Boundary: Characterisation at Tercis les Bains (France) and Correlation with Europe and Other Continents*. Developments in Palaeontology and Stratigraphy, vol. 19. Elsevier, Amsterdam, pp. 221–234.
- Schiøler, P., Brinkhuis, H., Roncaglia, L., Wilson, G.J., 1997. Dinoflagellate biostratigraphy and sequence stratigraphy of the Type Maastrichtian (Upper Cretaceous), ENCI Quarry, The Netherlands. *Mar. Micropaleontol.* 31, 65–95.
- Setoyama, E., Kaminski, M.A., Tyszką, J., 2011. Late Cretaceous agglutinated foraminifera and implications for the biostratigraphy and palaeobiogeography of the southwestern Barents Sea. In: Bubík, M., Kaminski, M.A. (Eds.), *Proceedings of the Eighth International Workshop on Agglutinated Foraminifera*, Cluj-Napoca, Romania, 7–13 September 2008. Grzybowski Foundation Special Publication: Kraków, Poland, 16, pp. 251–309.
- Setoyama, E., Radmacher, W., Kaminski, M.A., Tyszką, J., 2013. Foraminiferal and palynological biostratigraphy and biofacies from a Santonian–Campanian submarine fan system in the Vøring basin (offshore Norway). *Mar. Pet. Geol.* 43, 396–408. <https://doi.org/10.1016/j.marpetgeo.2012.12.007>.
- Setoyama, E., Kaminski, M.A., Tyszką, J., 2017. Late Cretaceous–Paleogene foraminiferal morphogroups as palaeoenvironmental tracers of the rifted Labrador margin, northern proto-Atlantic. In: Kaminski, M.A., Alegret, L. (Eds.), *Proceedings of the Ninth International Workshop on Agglutinated Foraminifera*. Grzybowski Foundation Special Publication 22, pp. 179–220.
- Slimani, H., 1995. Les dinokystes des craies du Campanien au Danien at Hallembaye et Turnhout (Belgique), et à Beutenaken (Pays-Bas): biostratigraphie et systématique. PhD thesis Research Unit Palaeontology Ghent University, Belgium, p. 461.
- Slimani, H., 2000. Nouvelle zonation aux kystes de dinoflagellés du Campanien au Danien dans le nord et l'est de la Belgique et dans le sud-est des Pays-Bas. *Memoirs of the Geological Survey of Belgium* 46, 1–88.
- Slimani, H., 2001. Les kystes de dinoflagellés du Campanien au Danien dans la région de Maastricht (Belgique et Pays-Bas) et de Turnhout (Belgique): biozonation et corrélation avec d'autres régions en Europe occidentale. *Geol. Palaeontol.* 35, 161–201.
- Slimani, H., Louwyse, S., Toufiq, A., 2010. Dinoflagellate cysts from the Cretaceous–Paleogene boundary at Ouled Haddou, Southeastern Rif, Morocco: biostratigraphy, paleoenvironments and paleobiogeography. *Palynology* 34, 90–124. <https://doi.org/10.1080/01916121003629933>.
- Slimani, H., Louwyse, S., Dussar, M., Lagrou, D., 2011. Connecting the Chalk Group of the Campine Basin to the dinoflagellate cyst biostratigraphy of the Campanian to Danian in borehole Meer (northern Belgium). *Neth. J. Geosci.* 90 (2–3), 129–164. <https://doi.org/10.1017/S0016774600001074>.
- Slimani, H., Guédé, K.É., Williams, G.L., Asebriy, L., Ahmamou, M., 2016. Campanian to Eocene dinoflagellate cyst biostratigraphy from the Tahar and Sekada sections at Arba Ayacha, western External Rif, Morocco. *Rev. Palaeobot. Palynol.* 228, 26–46. <https://doi.org/10.1016/j.revpalbo.2016.01.003>.
- Slimani, H., M'Hamdi, A., Uchman, A., Gasiński, M.A., Guédé, K.É., Mahboub, I., 2021a. Dinoflagellate cyst biostratigraphy of Upper Cretaceous turbiditic deposits from a part of the Băkowiec section in the Skole Nappe (Outer Carpathians, southern Poland). *Cretac. Res.* 123, 104780. <https://doi.org/10.1016/j.cretres.2021.104780>.
- Slimani, H., Benam, V.M., Țabără, D., Aassoumi, H., Jbari, H., Chekar, M., Mahboub, I., M'Hamdi, A., 2021b. Distribution of Dinoflagellate cyst assemblages and palynofacies in the Upper Cretaceous deposits from the neritic Bou Lila section, External Rif (northwestern Morocco): implications for the age, biostratigraphic correlations and paleoenvironmental reconstructions. *Mar. Micropaleontol.* 162, 101951. <https://doi.org/10.1016/j.marmicro.2020.101951>.
- Sluijs, A., Pross, J., Brinkhuis, H., 2005. From greenhouse to icehouse; organic-walled dinoflagellate cysts as paleoenvironmental indicators in the Paleogene. *Earth Sci. Rev.* 68, 281–315. <https://doi.org/10.1016/j.earscirev.2004.06.001>.
- Spezzaferri, S., Čorić, S., Hohenegger, J., Rögl, F., 2002. Basin-scale paleobiogeography and paleoecology: an example from Karpatian (Latest Burdigalian) benthic and planktonic foraminifera and calcareous nannoplankton from the Central Paratethys. *Geobios* 35, 241–256.
- Steffen, D., Gorin, G.E., 1993. Sedimentology of organic matter in Upper Tithonian–Berriasian deep-sea carbonates of Southeast France: evidence of eustatic control. In: Katz, B., Pratt, L. (Eds.), *Source Rocks in a Sequence Stratigraphic Framework: American Association Petroleum Geologists. Studies in Geology* 37, pp. 49–65.
- Țabără, D., Slimani, H., 2017. Dinoflagellate cysts and palynofacies across the Cretaceous–Paleogene boundary interval of the Vrancea Nappe (Eastern Carpathians, Romania). *Geol. Quart.* 61 (1), 39–52. <https://doi.org/10.7306/gq.1302>.
- Țabără, D., Slimani, H., 2019. Palynological and palynofacies analyses of Upper Cretaceous deposits in the Hațeg Basin, southern Carpathians, Romania. *Cretaceous Res.* 104, 104185. <https://doi.org/10.1016/j.cretres.2019.07.015>.
- Țabără, D., Slimani, H., Mare, S., Chira, C.M., 2017. Integrated biostratigraphy and palaeoenvironmental interpretation of the Upper Cretaceous to Paleocene succession in the northern Moldavidian Domain (Eastern Carpathians, Romania). *Cretac. Res.* 77, 102–123. <https://doi.org/10.1016/j.cretres.2017.04.021>.
- Țabără, D., Tudor, E., Chelariu, C., Olaru-Florea, R.F., 2021. Palaeoenvironmental interpretation and palynoflora of Devonian – Carboniferous subsurface sections from the eastern part of the Moesian Platform (Romania). *Rev. Palaeobot. Palynol.* 284, 104338. <https://doi.org/10.1016/j.revpalbo.2020.104338>.
- Țabără, D., Vasile, Ș., Csiki-Sava, Z., Bălc, R., Vremir, M., Chelariu, M., 2022. Palynological and organic geochemical analyses of the Upper Cretaceous Bozeș Formation at Petrești (southwestern Transylvanian Basin) – biostratigraphic and palaeoenvironmental implications. *Cretac. Res.* 134, 105148. <https://doi.org/10.1016/j.cretres.2022.105148>.
- Tahoun, S.S., Deaf, A.S., Ied, I.M., 2018. The use of cyclic stratigraphic pattern of peridinioid and gonyaulacoid dinoflagellate cysts in differentiating potential thick monotonous carbonate reservoirs: a possible ecostratigraphic tool under test. *Mar. Pet. Geol.* 96, 240–253. <https://doi.org/10.1016/j.marpetgeo.2018.05.030>.
- Thibault, N., Gardin, S., 2006. Maastrichtian calcareous nannofossil biostratigraphy and paleoecology in the Equatorial Atlantic (Demerara Rise, ODP Leg 207 Hole 1258A). *Rev. Micropaleontol.* 49, 199–214. <https://doi.org/10.1016/j.revmic.2006.08.002>.
- Thierstein, H.R., 1976. Mesozoic calcareous nannoplankton biostratigraphy of marine sediments. *Mar. Micropaleontol.* 1, 325–362.
- Thierstein, H.R., 1981. Late Cretaceous nannoplankton and the change at the Cretaceous–Tertiary boundary. *SEPM Spec. Publ.* 32, 355–394. <https://doi.org/10.2110/pec.81.32.0355>.
- Turculeț, I., 1971. *Inoceramus inconstans* Woods em. Studert, în *Stratele cu inoceramii de la Pîngărați (Unitatea de Tarcău)*. Lucrările Stațiunii "Stejarul" IV, Piatra Neamț.
- Tyson, R.V., 1995. *Sedimentary Organic Matter: Organic Facies and Palynofacies*. Chapman and Hall, London, p. 615.
- Vajda, V., Bercovici, A., 2014. The global vegetation pattern across the Cretaceous–Paleogene mass extinction interval: a template for other extinction events. *Glob. Planet. Chang.* 122, 29–49. <https://doi.org/10.1016/j.gloplacha.2014.07.014>.
- van der Zwaan, G.J., Jorissen, F.J., De Stigter, H.J., 1990. The depth dependency of planktonic/benthic foraminiferal ratios: constraints and applications. *Mar. Geol.* 95, 1–16. [https://doi.org/10.1016/0025-3227\(90\)90016-D](https://doi.org/10.1016/0025-3227(90)90016-D).
- Van Itterbeeck, J., Markevich, V.S., Codrea, V.A., 2005. Palynostratigraphy of the Maastrichtian dinosaur and mammal sites of the Râul Mare and Bărbat valleys (Hațeg Basin, Romania). *Geol. Carpath.* 56 (2), 137–147.
- Vellekoop, J., Kaskes, P., Sinnesael, M., Huygh, J., Déhais, T., Jagt, J.W.M., Speijer, R.P., Claeys, P., 2022. A new age model and chemostratigraphic framework for the Maastrichtian type area (southeastern Netherlands, northeastern Belgium). *Newsl. Stratigr.* <https://doi.org/10.1127/nos/2022/0703>.
- Waškowska, A., 2021. Agglutinated foraminiferal acmes and their role in the biostratigraphy of the Campanian–Eocene outer Carpathians. *Geosciences* 11, 367. <https://doi.org/10.3390/geosciences11090367>.
- Waškowska, A., Hnylko, S., Kaminski, M.A., Bakayewa, S., 2020. Grzybowski's Lviv Collection of Carpathian Foraminifera. Grzybowski Foundation Special Publication No. 25, Kraków, p. 169.
- Waškowska-Oliwa, A., 2003. Przegląd geologiczny. Biostratygrafia otwornicowa tufitów okna tektonicznego Wiśniowej. *Przegląd Geologiczny* 51, 261–262.
- Waškowska-Oliwa, A., 2005. Foraminiferal palaeodepth indicators from the lower Paleogene deposits of the Subsilesian Unit (Polish Outer Carpathians). *Studia Geologica Polonica* 124, 297–324.
- Waškowska-Oliwa, A., 2008. The Paleocene assemblages of agglutinated foraminifera from deep-water basin sediments of the Carpathians (Subsilesian Unit, Poland) -

- Biostratigraphical remarks. In: Hart, M., Kaminski, M.A., Smart, C. (Eds.), Proceedings of the Seventh International Workshop on Agglutinated Foraminifera. Grzybowski Foundation, Special Publication, Kraków, Poland, 13, pp. 227–265.
- Watkins, D.K., Self-Trail, J.M., 2005. Calcareous nannofossil evidence for the existence of the Gulf Stream during the Maastrichtian. *Paleoceanography* 20, 1–9. <https://doi.org/10.1029/2004PA001121>.
- Williams, G.L., Brinkhuis, H., Pearce, M.A., Fensome, R.A., Weegink, J.W., 2004. Southern Ocean and global dinoflagellate cyst events compared: index events for the late Cretaceous-Neogene. In: Exon, N.F., Kennett, J.P., Malone, M.J. (Eds.), Proceedings of the Ocean Drilling Program. Scientific Results 189, pp. 1–98.
- Williams, G.L., Fensome, R.A., MacRae, R.A., 2017. The Lentin and Williams index of fossil dinoflagellates, 2017 edition. AASP Contributions Series Number 48. American Association of Stratigraphic Palynologists Foundation, January 2017.
- Young, J.R., Bown, P.R., Lees, J.A., 2017. Nannotax3 Website. International Nannoplankton Association. <http://www.mikrotax.org/Nannotax3>.